J. theor. Biol. (2000) **204,** 257 – 288
doi:10.1006/jtbi.2000.2012, available online at http://www.idealibrary.com on IDEAL®

Mathematical Modelling of Nitric Oxide Activity in Wound Healing can explain Keloid and Hypertrophic Scarring

C. A. Cobbold* and J. A. Sherratt

Centre for Theoretical Modelling in Medicine, Department of Mathematics, Heriot-Watt University, Edinburgh EH14 4AS, U.K.

(*Received on* 28 *July* 1999, *Accepted in revised form on* 27 *January* 2000)

Keloid and hypertrophic lesions are both types of scarring pathologies which arise as a consequence of excess collagen deposition during the wound healing process. The exact mechanism by which this occurs is not understood and currently no effective treatment exists. In this paper, we study the possible role of nitric oxide in excess scar formation. In recent years, the physiological role of this free radical in mammalian tissue has been extensively studied; in particular numerous groups have studied its role in wound healing. We describe a mathematical model which offers a possible explanation for keloid scarring in terms of the presence of higher than normal nitric oxide concentrations related to the fact that nitric oxide stimulates synthesis of collagen by fibroblasts. As a consequence of this, we put forward a suggestion for a treatment strategy involving the surgical excision of the keloid lesion combined with the application of a low-dose nitric oxide inhibitor. In addition, we show that a quasi-steady-state analysis of our model reveals a possible approach to distinguishing between hypertrophic and keloid lesions, a task which has to date proven to be clinically difficult. We also present an extended model which confirms these results in the context of a more complicated and biologically more realistic system. The fuller model demonstrates additional features of keloid and hypertrophic scarring which we were not able to consider in the basic model, and as a consequence further supports our hypothesis that nitric oxide activity could play a key role in keloid scarring.

1. Introduction

Dermal wound healing is a complex process involving many overlapping stages, the end result frequently being a scar. The formation of a scar begins with the wound initially being closed by a blood clot (Asmussen & Sollner, 1993). Within about three days of injury, fibroblasts have begun migrating from the wound margins into the wound space where they eventually become the principal cell type (Leibovich & Ross, 1975). The fibroblasts gradually break down the blood clot, replacing it with a fibrous protein called collagen (Bauer & Uitto, 1982), the main structural protein of the skin. In parallel with this, immune cells migrate into the wound to remove any debris and foreign bodies. One of the dominant cells responsible for this are macrophages. They reach a maximum number around 3 days post-wounding (Leibovich & Ross, 1975), and we will focus on events that occur after this initial inflammatory stage.

Both macrophages and fibroblasts migrate into the wound in response to growth factors, in

* Author to whom correspondence should be addressed.
E-mail: c.a.cobbold@ma.hw.ac.uk, jas@ma.hw.ac.uk

0022–5193/00/100257 + 32 $35.00/0

particular transforming growth factor-β (TGF-β), which acts as a chemoattractant for both cell types (Wahl *et al*., 1987; Postlethwaite *et al*., 1987). The macrophage population size is almost solely a result of recruitment to the wound space (Riches, 1996), whereas fibroblasts also proliferate and this proliferation is enhanced by TGF-β (McCallion & Ferguson, 1996). There is also a positive feedback mechanism where fibroblasts and macrophages produce TGF-β (Roberts & Sporn, 1990). It is important to note that there are a number of other growth factors which have similar roles to TGF-β, but for the purposes of our model we shall focus on TGF-β as its importance has been made apparent by experimental data demonstrating its role in scar tissue formation (Sullivan *et al*., 1995; Shah *et al*., 1992).

The production of collagen by wound fibroblasts is also controlled in part by TGF-β (Roberts & Sporn, 1990), in combination with other regulators. In particular, nitric oxide also stimulates fibroblasts to produce collagen (Schaffer *et al*., 1997a), and in recent years this free radical molecule has become the focus of a number of wound-healing studies (Schaffer *et al*., 1997a; Lancaster, 1997). Nitric oxide (NO) is a very small molecule; so small that in fact it can pass through the membrane of a cell (Lisids *et al*., 1997). It is very reactive, with a half-life of the order of 5–15 s (Lancaster, 1997). It is well known as an environmental pollutant, present in cigarette smoke, smog and acid rain. However, in the 1980s it was discovered that mammalian cells produce nitric oxide, leading to a huge programme of experimental research on this molecule, which has proved to be crucial to many aspects of mammalian physiology. NO was found to have two main roles, firstly as a cell messenger and secondly as a cytotoxic agent (Lisids *et al*., 1997). Examples of these roles have been found in areas as diverse as neural signalling, immunocytotoxicity and regulation of vascular tone (Lisids *et al*., 1997). It is these last two on which we will focus in our consideration of the role of nitric oxide in wound healing.

The possible importance of nitric oxide in wound healing has already been demonstrated in a number of recent papers (Lancaster, 1997; Schaffer *et al*., 1997a). Data have shown that wound fibroblasts secrete nitric oxide, but normal fibroblasts do not (Schaffer *et al*., 1997a) and in particular, Schaffer *et al*. (1997b) provided experimental evidence of impaired healing occurring in the absence of NO. This provides a basis for wishing to consider such events in more detail. Nitric oxide is found to be predominantly produced by both fibroblasts and macrophages (Schaffer *et al*., 1997b). However, the production of this free radical by fibroblasts is inhibited by one of the other dominant chemicals involved in wound healing which we have discussed, namely, the cytokine TGF-β (Schaffer *et al*., 1997a).

Another key role for nitric oxide is its significant influence on vascular tone and as a result, NO affects the neovascularization phase of wound healing (Lisids *et al*., 1997). Thus, the free radical also affects oxygen concentration, firstly by increasing levels due to the blood vessel dilation, but also nitric oxide readily reacts with oxygen species (Lancaster, 1997), thus also decreasing the oxygen percentage in the wound. This aspect of healing is important since experimental data (McCallion & Ferguson, 1996) has indicated that the degree of hypoxia of the wound environment significantly affects the healing process.

Understanding the involvement and importance of nitric oxide in wound repair is of general interest; however further motivation for its study arises from an interest in two specific types of scarring pathology, that of hypertrophic and keloid scars. These scars are both characterized by excess collagen deposition (Tuan & Nichter, 1998) and hence the question arises: could nitric oxide levels account for the increased collagen? TGF-β levels remain similar to those found in normal wound healing (Younai *et al*., 1996), suggesting the collagen levels observed are not necessarily a result of TGF-β, thus leading us to consider nitric oxide.

Hypertrophic scars are confined to the wound area (Rockwell *et al*., 1989), while keloid scars affect both the wound and surrounding tissue (Rockwell *et al*., 1989). However in practice it is difficult to distinguish between the two. The more common hypertrophic case is often seen after burn injury, but as with keloids can also be a result of even very small dermal injury such as ear piercing and acne (Nemeth, 1993; Tuan & Nichter, 1998).

Keloid scarring is more common among darkly pigmented skin, with studies showing up to 16% of the population in some African communities being affected (Rockwell *et al*., 1989). Keloids consist of elevated fibrous growths; however unlike hypertrophic scarring these rarely regress (Peacock *et al*., 1970). They can be both painful and impair movement, and currently most treatments such as surgical removal are largely unsuccessful (Nemeth, 1993). In nearly all cases, keloids reoccur after therapy, whereas hypertrophic scars generally do not (Nemeth, 1993). So one clinical problem which has arisen from the difficulty in accurately distinguishing these scars is the possibility of incorrect treatment (Nemeth, 1993).

Biological differences between the two scar types suggest that nitric oxide levels could also be different. For instance, scar contracture and high levels of contractile fibroblasts (myofibroblasts) are seen in hypertrophic scars but not in keloids (Tuan & Nichter, 1998). Desmouliere *et al*. (1993) have indicated that TGF-β helps the transition of fibroblast to myofibroblast (Nodder & Martin, 1997), while NO suppresses it (Schaffer *et al*., 1997a). A natural hypothesis is that NO levels are higher in keloids. Studies done to date have not considered this issue, one possible reason being the fact that it is difficult to conduct experimental studies on keloids as they only occur in humans (Tuan & Nichter, 1998). So the aim of the mathematical modelling is to examine whether altered levels of this free radical could account for the two scars.

In the next section, we will proceed to derive a basic mathematical model capturing the main features of wound healing, focusing on the role of nitric oxide. In Section 3, we go on to carry out a quasi-steady-state analysis on our system. This enables us to locate the bifurcation point of the model, where the steady-state levels switch from cellular characteristics of a normal or hypertrophic scar to the acellular features of a keloid lesion. In Section 4, we proceed to numerically simulate our simple model and test the results of Section 3. In particular, we illustrate the characteristics of keloid and hypertrophic scars predicted previously. In Section 5, we use the analysis of Section 2 to characterize part of the model parameter space. This enables us to define the conditions under which we expect a particular type of scar to occur. We then extend our initial model to contain additional variables to improve the realism of our approach and to confirm the robustness of the model. Finally, in Section 7, we discuss our results with reference to biological data and comment on possible treatment strategies.

2. A Basic Mathematical Model

We begin with a simple mathematical model to allow us to focus on the effects of nitric oxide on the repair process. The model consists of four variables, considered on a time-scale starting approximately 20 days post-wounding. In contrast to previous wound-healing models (Olsen *et al*., 1995; Pettet *et al*., 1996) we concentrate on the remodelling stage of repair and consider the long-term outcomes. By focusing on events which occur after the proliferative phase we can neglect the effects of macrophages (Coleman *et al*., 1998; Haslett & Henson, 1996). We are also able to avoid including TGF-β as a variable because its main effects occur during inflammation (Coleman *et al*., 1998), where it is predominantly involved in cell chemotaxis and initial collagen production. Instead, we model the effects of the macrophages and growth factor in our initial conditions (Clark, 1996). We choose fibroblast cell density, $F(t)$ (cells mm^{-3}) and collagen density, $C(t)$ ($\times 5.4\ \mu\mathrm{g\,mg}^{-1}$ dry weight) as variables because they form the key components of the dermis (Clark, 1996); here t denotes time in days. Additionally, for the purposes of this study, collagen levels provide an indication of scarring pathology. For the third variable we have oxygen percentage, $O(t)$ (%), which allows us to model the degree of vasculature and hypoxia, both important aspects of wound healing (McCallion & Ferguson, 1996), and of particular interest in hypertrophic and keloid scarring. Oxygen also readily reacts with our main variable, nitric oxide, $N(t)$ (nM).

2.1. FIBROBLASTS

In modelling the fibroblast population, we represent the mitotic division of the cells by a logistic growth term. This assumption is supported by

the experimental data of Azzarone *et al.* (1983), who observed this behaviour while studying the population doublings of cultured fibroblast cell lines. Within this expression, we also include a crowding term representing the inhibitory effects of a dense collagen matrix on the rate of fibroblast proliferation (Clark, 1996). Finally, we have a linear decay term which models the natural death of the cell population. Included in this last term is a decreasing saturating function, $q(O)$, which represents the effects of hypoxia. The term hypoxia refers to oxygen levels of between 0 and 10%, whereas normal tissue has approximately 20% oxygen (Knighton *et al.*, 1983). There is little known about the exact mechanism by which oxygen affects fibroblast density (McCallion & Ferguson, 1996), but it is reasonable to assume that the cells are likely to have a shorter lifespan, with an impaired cell metabolism, in conditions of reduced oxygen, hence our choice of decreasing function. Combining these terms gives the following ordinary differential equation to represent the rate of change of fibroblast cell density:

$$\frac{\mathrm{d}F}{\mathrm{d}t} = F(1 - Fk_1 - Ck_2)r_1 - d_1Fq(O), \quad (1)$$

where

$$q(O) = \frac{p(1 + k_3) + O}{p + O}.$$

2.2. COLLAGEN

In our collagen equation, a first-order production term models the synthesis of the protein by fibroblasts. Schaffer *et al.* (1997a) demonstrated, via the exogenous addition of NO donors, that this collagen production is enhanced by moderate levels of nitric oxide, with high concentrations having cytoxic effects (Sarih *et al.*, 1993). Similar *in vitro* experiments by Witte *et al.* (1996) provided data which enabled us to obtain a qualitative approximation for this behaviour in the form of a function $g(N)$, as illustrated in Fig. 1. Although these data were for micromolar concentrations of nitric oxide, this general behaviour has been discussed in a number of papers (Schaffer *et al.*, 1997a; Lisids *et al.*, 1997; Sarih *et al.*, 1993), and experiments were nanomolar concentrations were used seem to coincide with these

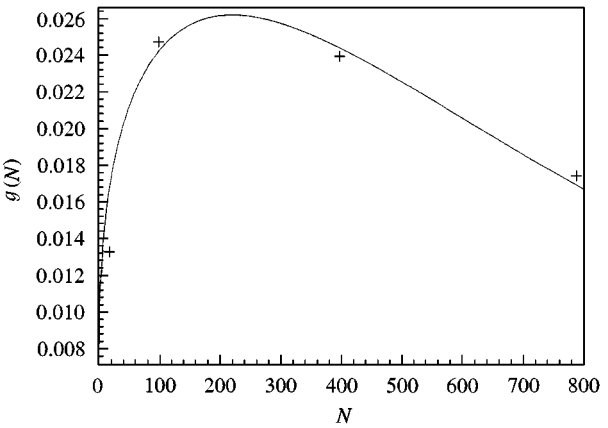

FIG. 1. Graph of the function $g(N)$, representing the dependence on nitric oxide of collagen production of fibroblasts. The graph is based on data from Witte *et al.* (1996) and illustrates the effects of nitric oxide concentration (μM) on the rate of collagen production. Low levels of NO give a moderate production rate and high levels have cytotoxic effects.

data, so that it is reasonable to assume that we can extend this result to nanomolar values. A carrying capacity function $h(C)$ is incorporated into the growth term to represent the crowding effects of high collagen density (Clark, 1996). Finally, we include a linear decay expression which depicts the breakdown and remodelling of collagen by fibroblasts (Clark, 1996). Together this gives

$$\frac{\mathrm{d}C}{\mathrm{d}t} = h(C)g(N)F - d_2CF \quad (2)$$

where $g(N)$ has the following form:

$$g(N) = \alpha + \beta N^{\gamma}\mathrm{e}^{\delta N}$$

and $h(C)$ has the qualitative behaviour as illustrated in Fig. 2.

2.3. OXYGEN

The conservation equation for oxygen consists of a first-order decay process modelling the reaction of oxygen with nitric oxide, and a general removal term which models the reaction of oxygen with other molecules. Oxygen is produced by blood vessels, so in this initial model we will assume that vasculature is at a constant level, v, which includes changes in effective vascular density caused by blood vessel occlusion. This can be

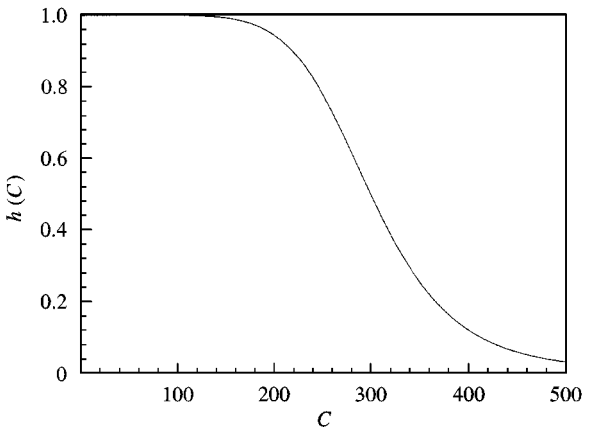

FIG. 2. Graph of the function $h(C)$, collagen carrying capacity function. The graph is based on clinical observations regarding collagen accumulation (Clark, 1996). The formation of excess scars leads us to the conclusion that a relatively high level of collagen is allowed to accumulate before the crowding effects come into play, hence the form of the graph above.

justified by the fact that we are considering the post-proliferative stage of the healing process (Clark, 1996), as it is during the proliferation phase that angiogenesis occurs. Thus, our production term consists of a constant linear growth term, the effects of which are enhanced further by nitric oxide which causes blood vessel dilation, thus increasing the rate of oxygen delivery (Lisids *et al.*, 1997). The dilation effect is represented by the increasing function, $s(N)$. There is a limit to the amount of dilation which can occur, so the function is chosen to saturate at a level k_5. Thus, we obtain the following equation:

$$\frac{\mathrm{d}O}{\mathrm{d}t} = k_4 v(1 + s(N)) - d_3 NO - d_4 O, \qquad (3)$$

where

$$s(N) = \frac{k_5 N}{N + k_6}.$$

2.4. NITRIC OXIDE

Finally, we have the conservation equation for nitric oxide. The decay terms are a result of the reactions of NO with oxygen, fibroblasts and the endothelial cells involved in blood vessel dilation as we described above (Haslett & Henson, 1996). We also include a background removal term which models the effects of other intermediate reactions involving this free radical. The main production term we will include is due to fibroblast cells (Schaffer *et al.*, 1997a); we assume this occurs at a constant rate, f_0 per cell. Other cells, such as endothelial cells, which produce nitric oxide in the dermis do so at a comparatively lower rate (Sarih *et al.*, 1993), with the exception of the macrophages involved in the inflammatory process. We will however include a constant production term, K, which models these contributions, so that we can assess its importance, particularly with regard to keloid and hypertrophic scarring. Thus, the final equation in our initial model is

$$\frac{\mathrm{d}N}{\mathrm{d}t} = Ff_0 - k_7 Nv(1 + s(N)) - d_5 N - d_6 FN - d_7 NO + K. \qquad (4)$$

2.5. INITIAL CONDITIONS

Finally, we choose the following initial conditions: $F(0) = F_0$, $C(0) = C_0$, $O(0) = O_0$ and $N(0) = N_0$. The values for F_0, C_0, O_0 and N_0 are based on approximations for the fibroblast, collagen, oxygen and nitric oxide levels at the end of the proliferative phase, although in the case of N_0, nitric oxide has such a small half-life (Lancaster, 1997) that the NO equation rapidly settles down to a quasi-steady state, independent of initial conditions.

3. Steady States

When investigating the steady states of our mathematical model, it is important to note that there is no equilibrium point corresponding to normal unwounded dermis. This is explained by the phenotypic alterations which occur to fibroblast cells in the wound. Normal fibroblasts from unwounded skin do not produce measurable amounts of nitric oxide, unless stimulated exogenously to do so (Witte *et al.*, 1996). However, the cells we model are wound fibroblasts, which have been shown to spontaneously synthesize NO both *in vitro* (Kirk *et al.*, 1993) and *in vivo* (Schaffer *et al.*, 1997a) within 24–72 hr post-wounding. This production of nitric oxide persists until the repair process is complete (Schaffer *et al.*, 1997a). For this reason, we cannot

obtain the unwounded steady state in our model as the fibroblasts considered have different characteristics to those of normal skin.

The homogeneous steady states for this system are difficult to derive explicitly, due to the complexity caused by functions such as $g(N)$. However, we can focus on a simpler problem, that of when the $F = 0$ steady state is stable. The motivation for considering this issue arises from our interest in keloid and hypertrophic scarring, and more specifically their biological characteristics. Keloid lesions consist of acellular nodes containing a high density of collagen, surrounded by microvessels which are either fully or partially occluded (Tuan & Nichter, 1998). Hypertrophic scars, on the other hand, are cellular and composed of aggregates of fibroblasts (Tuan & Nichter, 1998). Thus, the stability of the acellular equilibrium, $F = 0$, is a key question for the model.

To answer this question, we begin by making a quasi-steady-state assumption for the nitric oxide equation (4). This implies NO is at a constant level, $N = N_s$. This assumption is justified by noting that nitric oxide has a very fast production and removal rate, with time-scales of a minute or less (Wink *et al.*, 1996): this is extremely rapid when compared to the other events occurring in the system. In particular, fibroblasts have a cell cycle time of approximately 18–20 hr (Morgan & Pledger, 1992). Thus, on our time-scale of days we would expect nitric oxide to rapidly attain an equilibrium value. So NO concentration effectively becomes a parameter for our model. Using the assumption we obtain the following steady states:

(i)

$$F = 0,\ N = N_s,$$

$$O = \frac{k_4 v(1 + s(N_s))}{d_3 N_s + d_4} = O_s,\ C = C_s$$

(where C_s is arbitrary).

(ii)

$$F = \frac{1}{k_1}(1 - C_s k_2 - \frac{d_1}{r_1} q(O_s)) = F_s,$$

$$N = N_s,\ O = \frac{k_4 v(1 + s(N_s))}{d_3 N_s + d_4} = O_s,$$

$$\frac{C d_2}{g(N)} = h(C).$$

Recall that $h(C)$ is the collagen-carrying capacity function, so to simplify the problem further we assume $h(C) \approx 1$ which is justified by the fact that there are high collagen levels found in keloid and hypertrophic scarring (Rockwell *et al.*, 1989), and so it is unlikely that production rates are noticeably affected by collagen density. Therefore it is reasonable to neglect the effects of the carrying capacity function, $h(C)$.

As discussed earlier, the stability of these two quasi-steady state is of interest since the acellular $F = 0$ equilibrium could, under certain conditions, correspond to the biological characteristics of keloid lesions. By carrying out steady-state analysis on the reduced system, we obtain the stability matrix given by

$$M = \begin{pmatrix} -d_3 N - d_4 & 0 & 0 \\ -d_1 F q'(O) & (1 - 2k_1 F - k_2 C) r_1 - d_1 q(O) & -k_2 r_1 F \\ 0 & g(N) F - d_2 C & -d_2 F \end{pmatrix}_{O_s, F_s, C_s}$$

where O_s, F_s, C_s are the equilibrium points (i) or (ii) above.

If we consider the eigenvalues of M at the steady state given by (ii), we have the following:

$$\lambda_1 = -d_3 N - d_4 < 0; \quad \lambda_2 = -k_1 F_s r_1 < 0;$$

$$\lambda_3 = -d_2 F_s < 0.$$

As all the eigenvalues are negative it demonstrates that the cellular equilibrium (ii) is stable for $F = F_s \geqslant 0$, and this occurs when collagen levels satisfy $C \leqslant C_*$, where $C_* = (r_1 - d_1 q(O_s))/k_2 r_1$. By now focusing on the eigenvalues of M at

the steady state given by (i) we have

$$\lambda_1 = -d_3 N - d_4 < 0; \quad \lambda_2 = 0;$$

$$\lambda_3 = (1 - k_2 C_S) r_1 - d_1 q(O_S).$$

Thus, the stability of this equilibrium depends on the sign of λ_3. Hence, the acellular equilibrium (i) is stable for $C_s \geqslant C_*$, because we then have $\lambda_3 \leqslant 0$, and is unstable otherwise. So the system has a transcritical bifurcation, dependent on the nitric oxide concentration, as illustrated in Fig. 3(a).

Figure 3(a) demonstrates that at high enough levels of nitric oxide the acellular steady state becomes stable. Intuitively, this is a result of the high nitric oxide concentration leading to increased collagen production which reduces the extracellular space available for cell occupation. This is supported by examining the corresponding collagen equilibrium levels as illustrated in the bifurcation diagram in Fig. 3(b).

The two bifurcations diagrams illustrated show that at high nitric oxide concentrations, there is an increased level of collagen in a relatively acellular wound environment. This corresponds to biological characteristics of keloid scarring, and suggests that such histopathology is a result of high nitric oxide concentration. This hypothesis is supported by experimental observations by Tuan & Nichter (1998) which discuss the issue of contraction in such lesions. They found keloids to have few contractile fibroblasts, and Schaffer *et al.* (1997a) have shown that nitric oxide inhibits the phenotypic transition of fibroblasts to myofibroblasts. Hence, this also suggests the possibility of higher levels of NO in keloid scarring.

Russell & Witt (1976) have observed keloid and normal fibroblasts to have many of the same phenotypic characteristics. Therefore, given this similarity, we would not expect there to be a significant increase in the amount of NO released by keloid cells, although experimental data are lacking. So, in our model we would predict that any increased nitric oxide concentration is a result of the background production term K. A possible cellular source of this term is keratinocytes. In unwounded skin, the nitric oxide which keratinocytes produce is used as an intermediate

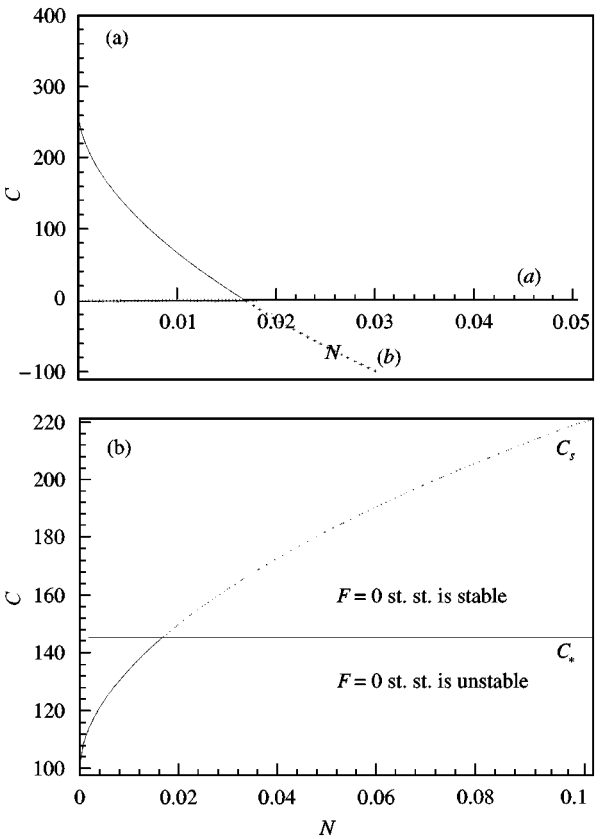

FIG. 3. (a) An illustration of the bifurcation diagram for the quasi-steady-state system, where nitric oxide concentration is at an equilibrium level $N = N_s$ (nM). Thus N effectively becomes a parameter for our model. The graph shows when the two steady states of this reduced system go from stable to unstable, specifically focusing on the fibroblast population, $F = F_s$ (cells mm^{-3}) as we vary nitric oxide concentration. The equilibrium (i) is an acellular state with $F_s = 0$ for all N. This is unstable (·····) for small to moderate N, but becomes stable (——) when the cellular state (ii) becomes unstable. Equilibrium (ii) is a cellular fibroblast state which remains stable as we increase $N = N_s$ until $F_s = 0$, at which point it becomes unstable to further increases in N. Figure 3(b) illustrates an alternative view of the bifurcation diagram, where we focus on the collagen density $C = C_s$ instead of the fibroblast levels. The line $C = C_s = g(N)/d_2$ is a graph of the collagen steady-state level associated with the cellular equilibrium (ii). The line $C = C_* = (r_1 - d_1 q(O_s))/k_2 r_1$ is a result of stability calculations which demonstrate that if $C > C_*$, the $F = 0$ steady state is stable and the cellular state is unstable in which case the collagen density is determined by initial conditions. For $C \leqslant C_*$, the $F \neq 0$ cellular equilibrium is stable, and the system evolves to collagen levels determined by C_s. So the $C = C_s$ steady state is stable (——) for small to moderate N and unstable (·····) for large N. The parameter values used here are: $r_1 = 0.924$, $d_1 = 0.116$, $d_2 = 0.000075$, $d_3 = 800$, $d_4 = 20$, $k_1 = 0.0004$, $k_2 = 0.006$, $k_3 = 0.5$, $k_4 = 5280$, $k_5 = 4$, $k_6 = 1.2$, $v = 7$, and the fibroblast density of normal unwounded dermis is $F_0 = 10$ cells mm^{-3}, with confluence occurring at 1000 cells mm^{-3} and the collagen level of unwounded skin is $C_0 = 100$ (536 μg mg^{-1} dry weight), with a normal scar having between a 20 and 30% increase in collagen density. These values are discussed further in Appendix A.

in the formation of the pigmentation chemical melain (Novellino *et al*., 1998). On wounding, melanocytes, the basal epidermal cells which produce melanin (Shier *et al*., 1996) are destroyed and not replaced (Shier *et al*., 1996), thus the nitric oxide which is normally used up in the pigmentation pathway is now free. Given that data concerning keloids show that this type of scarring is largely found in people with highly pigmented skin (Murray & Pinnell, 1992), we postulate that there is sufficient free nitric oxide available to fibroblasts to lead to the increased collagen production observed in keloids.

Also arising from our quasi-steady-state analysis is a possible explanation for hypertrophic scarring. Since this scarring pathology is cellular we would like to consider the $F \neq 0$ equilibrium. One supposition is that we have a high initial collagen level caused by the proliferative stage of healing and the system then regresses to the normal scarring steady state, which would match the spontaneous regression observed clinically (Ehrlich *et al*., 1994). This is something that we can investigate further in the numerical simulations of our model.

4. Numerical Simulations

Numerical simulations of our model [eqns (1)–(4)] were carried out using a stiff ODE solver. While investigating the system we were able to readily obtain simulations of normal scarring. We begin with a moderate level of fibroblasts, an order of magnitude higher than those found in normal skin. This corresponds to the influx of fibroblasts during the proliferative phase of the wound-healing process (Asmussen & Sollner, 1993). Similarly, we choose an initial collagen level in the same range as the unwounded dermis, and not exceeding the level detected in normal scarring, which is of the order of 120–130 ($\sim 690\,\mu g\,mg^{-1}$ dry weight) (Shah *et al*., 1992, 1994; Bardsley *et al*., 1995). This assumption is based on the experimental evidence concerning collagen deposition. It has been discussed by Jackson (1982) that collagen accumulates over the first 15–20 days post-wounding, which corresponds to the proliferative phase of repair.

With regard to our initial nitric oxide concentration, in the absence of experimental data we choose an arbitrary level. Generally, any reasonable choice of this initial condition has very little effect on the evolution of the system because of the rapid removal and production of this free radical, as discussed in the previous section. The oxygen percentage was chosen to be consistent with the hypoxia observed in healing wounds (Knighton *et al*., 1981), so we allow initial levels of between 0 and 10% in the simulation of normal scarring.

As predicted by our quasi-steady-state analysis, we were also able to obtain simulations of hypertrophic and keloid scarring. The initial conditions chosen to achieve these states were basically the same as those used to obtain the normal scarring illustrated in Fig. 4(a). This choice is based on the work by Peacock *et al*. (1970) and Murray & Pinnell (1992), who note few differences in the histopathology of these scarring types during the initial proliferative response to insult. However, when considering hypertrophic lesions, Schmid *et al*. (1998) have shown that hypertrophic fibroblasts exhibit an increased response to TGF-β. Therefore, we would expect a corresponding increase in collagen production to occur during the proliferative stage of repair. Hence, the resultant collagen levels from this phase are reflected in our initial conditions and so a higher initial collagen density is chosen in comparison to normal scarring. Moreover, numerical simulations suggest that this is an important factor in scarring.

There is contradictory evidence regarding the responsiveness of keloid fibroblasts to TGF-β (Babu *et al*., 1992; Bettinger *et al*., 1996), so for the purposes of this model we will assume keloid fibroblast cells respond to this cytokine in a similar way to normal wound fibroblasts. Thus, we choose initial collagen levels equivalent to those used to obtain normal scarring. This assumption is reasonable because if the system evolves to a keloid pathology under these conditions, then from the analysis in the previous section we would expect any higher initial collagen concentration to lead to a more severe keloid scar.

As well as initial conditions, the biological differences between normal, hypertrophic and keloid scarring lead to corresponding parameter differences. In particular, Wang *et al*. (1997) have observed that human hypertrophic fibroblasts

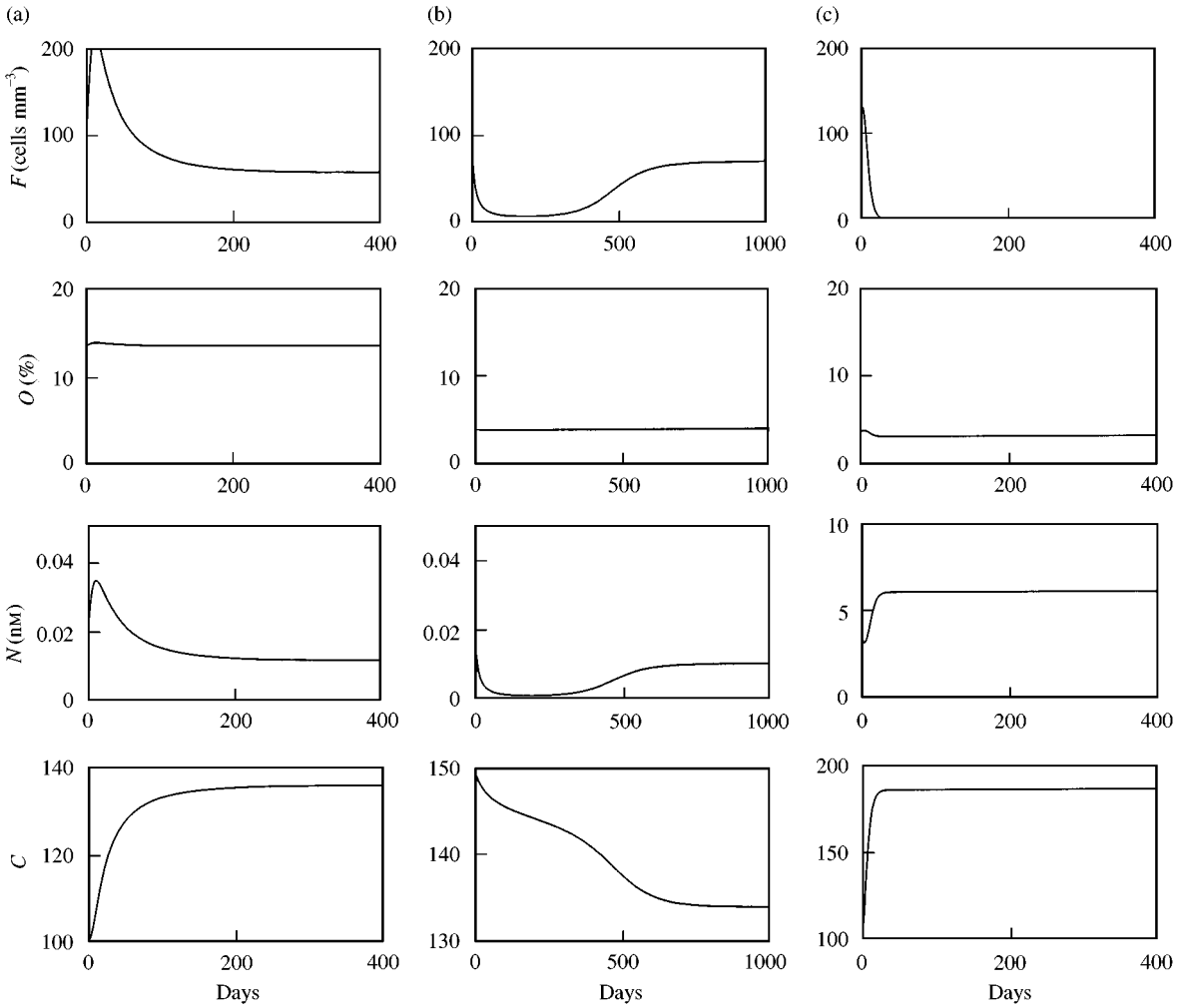

FIG. 4. Numerical simulations of our model [eqns (1)–(4)] illustrating normal, hypertrophic and keloid scarring. Column (a) shows the characteristics of normal scarring, for example the 30% increase in collagen levels in comparison to the unwounded dermis (~ 100). This corresponds to biological data on scar tissue (Shah *et al.*, 1992, 1994; Bardsley *et al.*, 1995). The initial conditions used are: $F(0) = F_0 = 100$ cells mm^{-3}, $C(0) = C_0 = 100 \times 5.4$ μg mg^{-1} dry weight, $N(0) = N_0 = 1$ nM and $O(0) = O_0 = 0\%$. The parameter values used are as follows: $r_1 = 0.92$, $d_1 = 0.12$, $d_2 = 0.000075$, $d_3 = 800$, $d_4 = 3800$, $d_5 = 500$, $d_6 = 20$, $d_7 = 800$, $k_1 = 0.0004$, $k_2 = 0.006$, $k_3 = 0.5$, $k_4 = 5280$, $k_5 = 4$, $k_6 = 1.2$, $k_7 = 185$, $v = 7$, $a_1 = 1/300$, $m = 20, f_0 = 2.79$, $K = 0$. These values are discussed further in Appendix A. Column (b) illustrates the excess scarring seen in hypertrophic lesions. The fibroblast graph shows an increased cellularity [cf. with Fig. 4(a)] and collagen levels show the gradual regression of the scar. Parameters are the same as those used for normal scarring (a) with the exception of $v = 1$, $f_0 = 0.79$. Initial conditions remain the same except for: $C(0) = C_0 = 149$ ($\times 5.4$ μg mg^{-1} dry weight). Column (c) illustrates keloid scarring. In contrast to (b) the fibroblast levels show an acellular wound. The oxygen levels correspond to hypoxia ($< 10\%$) and we have a very high density of collagen (a two-fold increase on normal tissue) with a corresponding high level of nitric oxide. Parameters and initial conditions are as in (a) except for $v = 1$, $K = 20\,000$.

in vitro secrete significantly lower levels of nitric oxide compared to normal wound fibroblasts. In terms of our model, this implies a smaller value of f_0 in our NO eqn (4). In order to simulate keloid scarring, we allow a larger background nitric oxide production rate, K. This is to reflect our hypothesis that higher NO concentration may lead to forms of excess scarring. Further justification of this term was discussed in the previous section. The remaining parameters are estimates taken from biological data and are discussed in more detail in Appendix A. Hence, Fig. 4(b) illustrates hypertrophic scarring and Fig. 4(c) shows the pathology of keloid lesions.

Figure 4 demonstrates the main characteristics of the three scarring phenotypes we have been

considering. In the case of normal scarring in Fig. 4(a), we observe that the system settles down to collagen concentrations approximately 30% higher than normal unwounded dermal levels (~ 100), which is consistent with experimental data from Shah *et al.* (1992, 1994) and Bardsley *et al.* (1995). In parallel with this, the oxygen levels have recovered from their hypoxic state and cell numbers have evolved to an equilibrium only slightly higher than that found in the normal dermis ($\sim 10\,\text{cell}\,\text{mm}^{-3}$). These are all features consistent with the normal scarring pathology. The hypertrophic lesions illustrated in Fig. 4(b) capture the main biological characteristics observed clinically. In particular, the resultant scar is more cellular than normal scar tissue (Rockwell *et al.*, 1989), with approximately a two-fold increase in fibroblast density. One of the key histological features demonstrated by this model is the spontaneous regression frequently associated with hypertrophic scars. In our model, this regression period is the time taken for the system to settle down to a steady state. The simulations demonstrate that it can take up to 2.5 yr to regress, which is consistent with clinical observations of regression times between 1 and 3 yr (Nemeth, 1993). In the simulations, different regression times can also be seen by changing the initial collagen levels, C_0. This parameter change reflects different degrees of responsiveness to TGF-β during the proliferative phase of wound healing. If C_0 and f_0 are high enough, non-regressing hypertrophic scars are observed, which have characteristics of both keloid and hypertrophic lesions. Such cases are found clinically (Blackburn & Cosman, 1966) and this contributes to the difficulty which exists in distinguishing between scar types.

Finally, Fig. 4(c) depicts keloid scarring. The key features of this case include its acellular nature, hypoxic environment and high collagen density, which is double that of normal skin. Also, as described clinically (Ehrlich *et al.*, 1994), no regression is observed. The main result we obtain from this simulation is the conclusion that different nitric oxide levels could account for keloid scarring, particularly given that Fig. 4(c) shows significantly higher nitric oxide concentrations in comparison to those found in normal and hypertrophic scar tissue.

The results we have obtained from our model suggest that a keloid lesion would appear approximately 3 months after the injury [this is based on assuming the proliferative phase ends at around 25 days post-wounding (Asmussen & Sollner, 1993)]. This scale corresponds to some of the clinical observations (Murray & Pinnell, 1992; Peacock *et al.*, 1970), but certainly there is numerous data to suggest that it frequently takes of the order of 1 yr for the scar to appear (Nemeth, 1993). This can be readily explained in our model by considering our constant nitric oxide production term K. In our simulations, we assume that at the end of the proliferative phase the full effects of the background production of nitric oxide begin. Biologically, this may be unrealistic and the effects are likely to be more gradual; as a consequence there would be a much longer period post-wounding before the appearance of a keloid lesion. This is an aspect of our model which we could expand on in future work, focusing in particular, on the source of this background NO. However, for an initial model, it is the qualitative features that are our main focus. In particular, clinical interest in distinguishing between scar types (Nemeth, 1993) leads us to consider the possible division of the parameter space into regions which characterize the different scarring pathologies, which we proceed to do in the next section.

5. Characterizing Scar Types

Characterizing the parameter space for our model provides a method of distinguishing between scar types, which is something which could be of particular clinical use. The key parameters which we will focus on are the initial collagen level, C_0; f_0, the rate fibroblasts produce nitric oxide, and finally the rate of background nitric oxide production, K. The particular importance of these three parameters has been made evident by our quasi-steady-state analysis, numerical simulations and biological studies. The initial collagen level, C_0 for example, is an indication of the collagen concentration at the end of the proliferative phase and reflects the sensitivity of fibroblasts to TGF-β. So, this parameter may have biological significance in classifying hypertrophic lesions, because experimental data of

Schmid *et al.* (1998) show that hypertrophic fibroblasts have an increased responsiveness to TGF-β. In addition to this, our analysis and simulations suggest that the value of C_0 could be key in determining whether scar regression is possible, and such regression is a characteristic feature of hypertrophic scars (Nemeth, 1993; Ehrlich *et al.*, 1994). Similarly, our motivation for considering f_0 arises from observed (Wang *et al.*, 1997) *in vivo* differences in this parameter value, between normal and hypertrophic fibroblasts. The value of f_0 is also important in determining the nitric oxide equilibrium, and is therefore of further interest.

Finally, the background nitric oxide production rate, K, is of importance because of our hypothesis that higher NO concentration could account for excess scarring, in particular the keloid pathology. K is the main parameter which determines the nitric oxide steady-state level, N_s, and as discussed in our quasi-steady-state analysis, the NO concentration is significant in determining whether the system evolves to a cellular or acellular state; the acellular state being a feature of keloid scars (Blackburn & Cosman, 1966; Appleton *et al.*, 1996). Thus, we can regard the nitric oxide production rate, K, as a measure of N_s. To distinguish between hypertrophic and normal scarring we begin by focusing on the C_0–f_0 parameter space. Both these types of scar are cellular so we need to consider the case when the fibroblast equilibrium, $F = F_s \neq 0$ is stable. As we have seen in Section 3 this corresponds to when the collagen steady state $C_s \leqslant C_* = (r_1 - d_1 q(O_s))/k_2 r_1$. Thus if our initial collagen level $C_0 > C_*$, our quasi-steady state analysis in Section 3 implies that the system would evolve to the acellular equilibrium and hence to a keloid type scar. The conclusion has also been confirmed in numerical simulations (not shown). So we now concentrate on the initial collagen concentrations such that $C_0 < C_*$. In this region, there is only one stable steady-state level $C_s = g(N)/d_2$ for collagen (taking the approximation from Section 3 that $h(C) \approx 1$), and thus density evolves to this level. However, if we have $C_0 > C_s$, i.e. a high fibroblast sensitivity to TGF-β, we would have excess scar tissue, C_0 which would regress down to normal scar levels, C_s, as demonstrated by the simulations in Fig. 4(b).

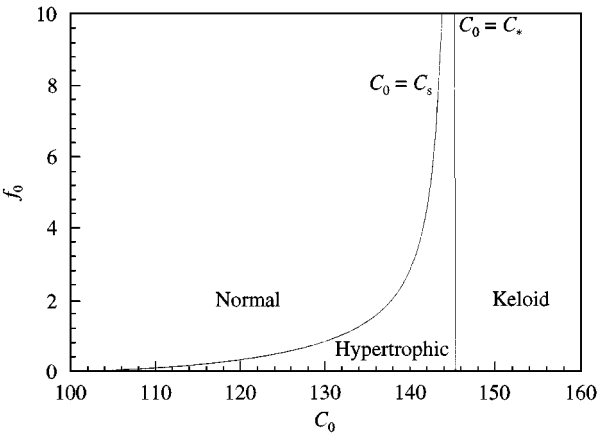

FIG. 5. Division of the C_0–f_0 parameter space to characterize the three scarring phenotypes: normal, hypertrophic and keloid scars. C_0 is the resultant collagen levels at the end of the proliferative phase and is a measure of fibroblast sensitivity to TGF-β. f_0 is the rate at which fibroblasts produce nitric oxide, a value which is known to vary between scar types. The graph demonstrates that if C_0 is such that $C_0 > C_s$ then hypertrophic lesions may be observed. Here, C_* is the collagen level corresponding to when the acellular state becomes stable. Thus, $C_0 > C_*$ implies that a keloid lesion will occur. C_s is the collagen equilibrium associated with the cellular state, so if $C_0 < C_s$, the system will evolve to C_s and a corresponding normal scar will form. Parameter values used here are as in Fig. 3(a), with $K = 0$.

So this provides some criteria to categorize hypertrophic lesions and normal scars.

In addition, we need to consider the role of f_0 in the characterization of these scar types. We have already seen that nitric oxide concentration affects the evolution of our model and determines the collagen concentration, C_s. Since N_s is dependent on the rate at which fibroblasts produce nitric oxide, it follows that f_0 affects C_s. As demonstrated in our graph of the C_0–f_0 parameter space in Fig. 5, for a fixed background production, K, low values of f_0 lead to corresponding decreases in C_s. Given that C_* is a fixed value, independent of f_0 and K, it follows that there could be a large difference between C_* and C_s for small f_0. This implies that in this case there is an increased chance of longer regression times, particularly if C_0 takes a value close to C_*. This conclusion is supported by Wang *et al.* (1997), whose study showed a significantly lower value for the rate at which fibroblasts synthesize nitric oxide in hypertrophic tissue. We also note that Fig. 5 illustrates that high values of f_0 are

accompanied by steady-state collagen levels, C_s which are very close to C_*. This suggests that a more severe scar is formed, or may even be regarded as a non-regressing hypertrophic lesion. All these features are illustrated in Fig. 5, in our plot of the C_0–f_0 space.

Figure 5 is obtained by taking a fixed value of K. The qualitative features continue to hold as we increase K to K_*, with the value of C_s at $f_0 = 0$ increasing to C_*. The curve $C_0 = C_s$ moves towards the line $C_0 = C_*$, and biologically, this implies that increased background nitric oxide causes higher levels of collagen in the normal scar, and shorter regression times in the hypertrophic lesions, so that the resultant scar looks increasingly like a keloid. Such cases have been observed clinically, and patients have been found to have scars which exhibit features of both the hypertrophic and keloid scar (Blackburn & Cosman, 1966; Ehrlich *et al*., 1994). In the study by Blackburn & Cosman (1966), such lesions were categorized by several different independent pathology groups in order to obtain more accurate results, but the conclusions from all groups remained fairly consistent, and described this "intermediate" type of scar.

We note that in Fig. 5 keloids are categorized as occurring when the initial collagen concentration $C_0 > C_*$. Although this would give some of the characteristics of keloid lesions, such as its acellularity, biologically this is unlikely to be the source of this scarring because it implies a high fibroblast sensitivity to TGF-β and this would suggest the presence of myofibroblasts (Desmouliere *et al*., 1993), and these are found to be absent in keloids (Jackson, 1982; Tuan & Nichter, 1998). Instead keloids are more likely to occur as a result of high nitric oxide concentrations as they can occur in the entire (C_0–f_0)-parameter space when $K > K_*$ (this corresponds to the NO level being such that $N_s > N_*$). As we have seen in Section 3, this condition results in $C_s \geqslant C_*$ and the $F_s = 0$ acellular equilibrium being stable, and clinical evidence associates such features with the keloid pathology (Blackburn & Cosman, 1966; Appleton *et al*., 1996). It is more likely that keloids arise as a result of this high nitric oxide concentration because it can account for the absence of contractile fibroblasts in these lesions. This is due to the fact that TGF-β has been suggested to stimulate the phenotypic change of fibroblast to myofibroblasts (Desmouliere *et al*., 1993) and nitric oxide has been implicated in inhibiting such a transition (Schaffer *et al*., 1997a).

So far our results and analysis point strongly towards a role for nitric oxide in excess scarring. Figure 5 demonstrates that by measuring just three parameters, K, C_0 and f_0, we should be able to classify the scar type and hence treat accordingly. However, at this point the conclusions come from our simple model, so in order to clarify some of these hypotheses and to test the robustness of the model, in the next section we will check the predicted behaviour in a fuller system, which captures more of the features of the actual biological situation.

6. Full Model

In order to obtain a more realistic mathematical model of the wound-healing process, we extend our first system of equations to include some of the biological factors we discussed in the introduction. In particular, we introduce the following additional variables: macrophage density, $M(t)$ cells mm^{-3}, TGF-β concentration, $T(t)\,10^{-2}$ ng mm^{-3}, and blood vessel density, $V(t)$. $V(t)$ will be regarded as a notional variable and is dimensionless, because any attempt to give units to $V(t)$ would require including additional variables such as capillary sprout density. Our time variable, t, is still measured in days, but the introduction of inflammatory cells, namely macrophages, leads us to consider $t = 0$ as now representing the point of inflammation, which occurs approximately 3 days post-wounding when fibroblasts first appear (Leibovich & Ross, 1975).

The rationale for including these three variables is made evident in our introduction. For example, TGF-β is perhaps one of the most multifunctional cytokines found during wound healing (Roberts & Sporn, 1996) and numerous studies have demonstrated its importance in scar tissue formation (Sullivan *et al*., 1995). In parallel with this, we include macrophages as they are a major source of TGF-β (Sullivan *et al*., 1995) and nitric oxide (Schaffer *et al*., 1997a), and studies have demonstrated that macrophage absence leads to impaired healing (Leibovich & Ross,

1975; Knighton & Fiegel, 1989). Finally, blood vessel density is represented because of the well-documented effect of nitric oxide on angiogenesis (Ku, 1996; Lisids *et al*., 1997), and its clear role in controlling tissue hypoxia. Also, further interest arises as a result of experimental evidence which has found that hypertrophic and keloid tissue is more vascularized than normal scar tissue (Ehrlich *et al*., 1994), although in both cases the microvessels are either partially or fully occluded (Kischer *et al*., 1982).

The equations for our additional variables are given by

$$\text{Macrophages:}\quad \frac{\mathrm{d}M}{\mathrm{d}t} = \overbrace{k_8 T}^{\substack{\text{influx due to}\\ \text{chemotactic migration}}} - \overbrace{d_8 M}^{\substack{\text{natural}\\ \text{decay}}}. \tag{5}$$

$$\text{TGF-}\beta\text{:}\quad \frac{\mathrm{d}T}{\mathrm{d}t} = \overbrace{TMk_9}^{\substack{\text{production by}\\ \text{macrophages}}} + \overbrace{FTk_{10}}^{\substack{\text{production by}\\ \text{fibroblasts}}} - \overbrace{d_9 T}^{\substack{\text{natural}\\ \text{decay}}}. \tag{6}$$

$$\text{Blood vessels:}\quad \frac{\mathrm{d}V}{\mathrm{d}t} = \overbrace{k_{11} MV}^{\substack{\text{angiogenesis}\\ \text{due to MDGF}}} \overbrace{\left(1 - Vk_{12} - \frac{Ck_{13}}{1 + Ck_{13}}\right)}^{\substack{\text{growth restriction due to}\\ \text{collagen \& blood vessels}}} \overbrace{l(O)}^{\substack{\text{growth due}\\ \text{to hypoxia}}}. \tag{7}$$

The macrophage population arises almost entirely as a result of chemotactic migration into the wound space (Riches, 1996), and TGF-β is the principal chemoattractant for this behaviour (Riches, 1996), hence the choice of production term in eqn (5). With regard to the conservation of TGF-β [eqn (6)], the peptide growth factor is largely produced by macrophages and fibroblasts. However, TGF-β has an autocatalytic behaviour and so also stimulates its own synthesis, as represented by our equations. Lastly, blood vessel growth [eqn (7)] or angiogenesis has been shown to be caused by macrophage-derived growth factors (MDGF) released by macrophage cells (Knighton & Fiegel, 1989). This behaviour is regulated by the oxygen microenvironment and indeed the degree of hypoxia (Knighton & Fiegel, 1989). Results of Knighton & Fiegel (1989) suggest that macrophages combined with the hypoxic wound space are required to produce neovascularization. Knighton *et al.* (1983) support this with data indicating that normal tissue conditions of 20% oxygen resulted in no angiogenic response. With 5–10% oxygen, activity was seen, but it was not substantial. Only at the more severe hypoxic state of 2% oxygen did macrophages cause substantial stimulation of blood vessel growth. If we incorporate this behaviour into a function, $l(O)$ say, we obtain the qualitative form, as illustrated in Fig. 6.

Combining these various features gives eqns (5)–(7). The differential equations describing the remaining variables are just an extension of our original model, and these are given by eqns

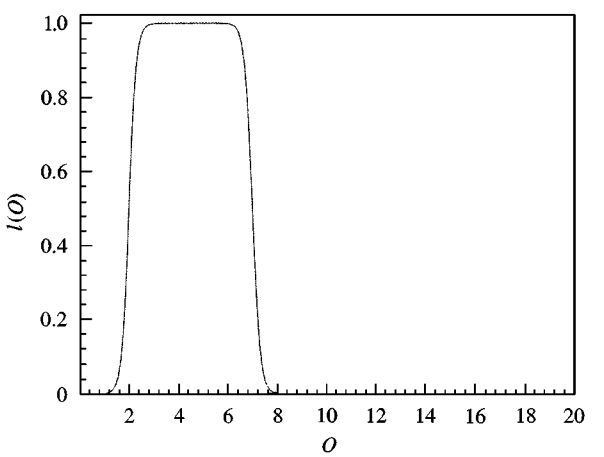

FIG. 6. Graph of the function $l(O)$, which represents the effects of oxygen percentage, $O(t)$, on neovascularization. The form of the graph shows that oxygen levels of normal tissue (20%) or higher correspond to no angiogenic activity, while wound hypoxia of between 2 and 7% leads to maximal stimulation of blood vessel growth. Data for this function comes from Knighton *et al.* (1983).

(8)–(11), where the boxes indicate new terms:

$$\text{Fibroblasts:}\quad \frac{\mathrm{d}F}{\mathrm{d}t} = F(1 - Fk_1 - Ck_2)(r_1 + \overbrace{\boxed{r_2T}}^{\substack{\text{proliferation}\\ \text{due to TGF-}\beta}}) - d_1Fq(O), \tag{8}$$

$$\text{Collagen:}\quad \frac{\mathrm{d}C}{\mathrm{d}t} = g(N)Fh(C) + \overbrace{\boxed{k_{16}TFh(C)}}^{\substack{\text{production by fibroblasts}\\ \text{in response to TGF-}\beta}} - d_2CF, \tag{9}$$

$$\text{Oxygen:}\quad \frac{\mathrm{d}O}{\mathrm{d}t} = k_4V(1 + s(N))(\overbrace{\boxed{1 - u(M,N)}}^{\substack{\text{blood vessel}\\ \text{occlusion}}}) - d_3NO - d_4O - \overbrace{\boxed{d_{10}Ml(O)}}^{\substack{\text{reaction with}\\ \text{macrophages}}} \tag{10}$$

$$\text{Nitric oxide:}\quad \frac{\mathrm{d}N}{\mathrm{d}t} = \overbrace{\boxed{k_{15}M}}^{\substack{\text{production by}\\ \text{macrophages}}} + \overbrace{\boxed{Ff(T)}}^{\substack{\text{prod}^{n}\text{ by fibroblasts with}\\ \text{inhibition by TGF-}\beta}} - k_7NV(1 + s(N))(\overbrace{\boxed{1 - u(M,N)}}^{\substack{\text{blood vessel}\\ \text{occlusion}}}) - d_5N - d_6FN - d_7NO + K. \tag{11}$$

Here,

$$u(M, N) = \frac{M}{M + k_{14}} + \frac{N}{N + k_{17}}$$

and recall

$$s(N) = \frac{k_5N}{N + k_6}.$$

The equation describing the fibroblast population [eqn (8)] now incorporates the effects of the cytokine TGF-β. Numerous studies have found that TGF-β is indirectly a mitogen for fibroblast cells (Liu & Connolly, 1998), hence the growth rate r_1 is adapted accordingly. Similarly, the collagen differential equation includes an additional production term which is due to TGF-β-stimulating fibroblast cells to synthesize collagen.

To model the oxygen concentration $O(t)$, we modified our simple system by replacing the constant v, which models degree of patent vasculature with the variable $V(t)$. This is because angiogenesis reaches its peak after 3–7 days post-wounding (Asmussen & Sollner, 1993) and almost entirely occurs during the proliferative phase of healing (Nissen *et al.*, 1998), and it is this stage that we are now including. We also introduce the effects of occlusion caused by the overproliferation of endothelial cells (Kischer *et al.*, 1982). This feature is caused by macrophage-derived angiogenic factors, and its effect is to reduce the size of the blood vessel lumen and thus to lower the oxygen released by the vasculature (Knighton *et al.*, 1981). Fukuo *et al.* (1995) have shown that excess endothelial cell proliferation is also indirectly caused by high levels of nitric oxide. This occurs via high NO concentrations inducing vascular smooth muscle cell damage, these damaged cells then release basic fibroblast growth factor which stimulates endothelial cell proliferation. Thus, we represent the resultant macrophage and nitric oxide-induced occlusion by an increasing function, $u(M, N)$, and since the oxygen levels decrease as the vessels become less patent, the term which appears in our model [eqn (10)] takes the form $1 - u(M, N)$. Lastly, we have an extra decay term which represents the removal of oxygen as a result of the reaction with macrophage-derived growth factors.

With regard to the nitric oxide equation (11), the term representing removal by blood haemoglobin is modified in the same manner as the oxygen production term. We change the nitric oxide production expression to now include the effects of TGF-β on fibroblast synthesis of NO. Schaffer *et al.* (1997a) have demonstrated that this cytokine inhibits the production of NO by

fibroblasts. There is currently no evidence regarding the mechanism by which this occurs, so consequently we choose a functional form, $f(T)$, which represents the general behaviour observed. For simplicity, we have chosen an exponential decay function, with $f(0) = f_0$ from our previous model. Finally, there is an additional production term representing NO produced by macrophages; this is one of the principal sources of the free radical and data have shown macrophages release nitric oxide at a rate which is over 3 times greater than that of fibroblasts, the other main source. These alterations lead us to our full model [eqns (5)–(11)], which we will now investigate. With regard to the parameter values, in the case of the simple model they were based on experimental data and are reasonably well known; however, this fuller model has parameter values based more on order of magnitude approximations as there is an absence of exact data. This is discussed in more detail in Appendix A.

6.1. NUMERICAL SIMULATIONS OF THE FULL MODEL

Now that we have set up a more detailed model [eqns (5)–(11)] we use the stiff ODE solver described in Section 2 to generate numerical simulations of this system. The initial conditions used to demonstrate all the types of scarring we discuss are essentially the same. The rationale for this comes from a number of studies which hypothesize that the initial phases of the repair process are very similar, with morphological differences only appearing after the proliferative stage (Peacock *et al*., 1970; Blackburn & Cosman, 1966). The initial conditions consist of a low level of collagen, C_0 of the order of 0–10 ($\times 5.4\ \mu g\, mg^{-1}$ dry weight). This is because, by 3 days post-wounding ($t = 0$), fibroblasts are in the process of migrating into the wound space (Leibovich & Ross, 1975) and studies show that collagen production maximally occurs after the cell migration (McCallion & Ferguson, 1996). We can justify this choice further by noting that if the system evolves to an excess scar as a result of an underestimation of C_0, then we would certainly expect higher values of this parameter to also lead to an excess scar.

The density of fibroblast cells at $t = 0$ is chosen to be of a moderate level, but higher than that of the unwounded dermis ($\sim 10\ cells\, mm^{-3}$) (Shah *et al*., 1992, 1994; Bardsley *et al*., 1995). The basis for this choice comes from recent data which suggest a significant number of cells would have infiltrated the wound by day 3, with fibroblasts reaching a maximal level a few days later, at approximately 5–7 days post-wounding (Adams, 1997). The initial oxygen percentage, $O(0) = O_0$ corresponds to the hypoxia found in the wound dead space. Thus, a value is chosen between 0 and 5%.

As we have discussed in the numerical simulations of the simple model, the initial nitric oxide level has a negligible effect on the evolution of the system due to the high reactivity of this free radical (Lancaster, 1997); thus we chose an arbitrary, but reasonable NO concentration. With respect to macrophage cells, Leibovich & Ross (1975) demonstrated that they reach maximal numbers approximately 72 hr after injury ($t = 0$). Hence, the value of $M(0) = M_0$ has been taken to be of the order of $100\ cells\, mm^{-3}$ (Leibovich & Ross, 1975; Wahl *et al*., 1987). Related to this is the initial concentration of TGF-β. We would expect the level to be reasonably high given that macrophages are at a maximum level and the degranulation of platelets has been extensive by this point, and associated to this is the release of significant quantities of TGF-β (Roberts & Sporn, 1990). Thus, data would suggest levels would certainly be of at least the order of $1–10 \times 10^{-2}\ ng\, ml^{-1}$ (Wahl *et al*., 1987). The initial blood vessel density is much more difficult to estimate as we are regarding $V(t)$ as a notional variable. Consequently, we choose an arbitrary value for $V(0) = V_0$, and to access the degree of vascularization of the resultant scar we compare the steady-state values to those given by the numerical simulation of normal scarring, by assuming that this has average blood vessel density.

Using these estimates for initial conditions, we were able to generate numerical simulations of normal, hypertrophic and keloid scarring. This was achieved by altering those parameters which have been observed experimentally to vary be tween scar types. The resulting simulations are illustrated in Fig. 7. Figure 7 confirms that the three scarring phenotypes we have been considering can also be produced in a fuller model. This

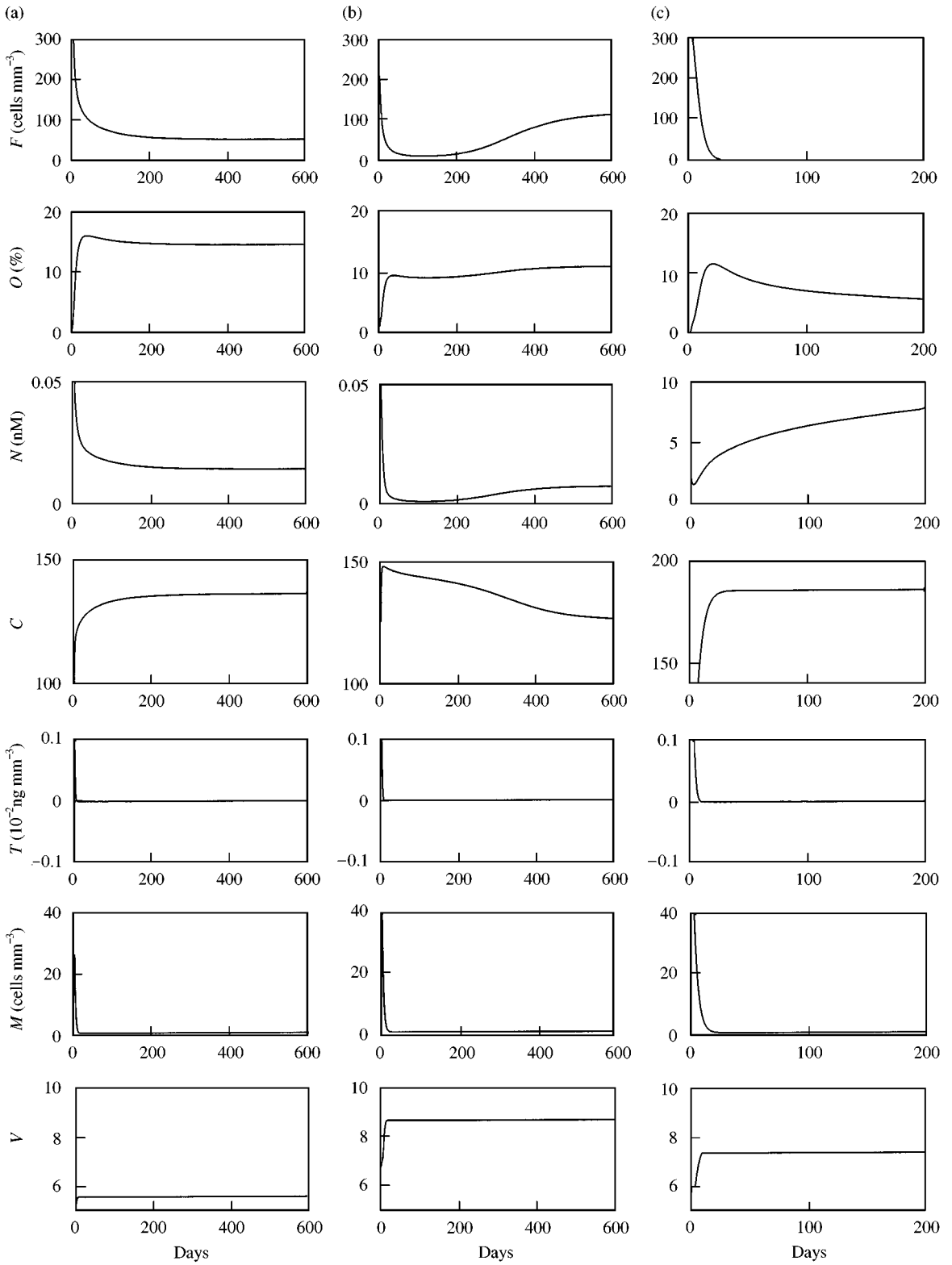

FIG. 7. (*Caption opposite*)

helps to confirm the robustness of our simple model and consequently supports the hypotheses and analysis carried out in the previous sections. Figure 7(a), which demonstrates normal scar tissue, evolves to steady-state levels which are consistent with our results in Section 4. Thus, corresponding to experimental results (Shah *et al*., 1992, 1994; Bardsley *et al*., 1995), approximately a 30% increase in collagen density was found, where normal unwounded tissue is ~ 100 ($\times 5.4\ \mu g\, mg^{-1}$ dry weight). With regard to the additional variables in our modified model, both TGF-β and macrophages evolve to negligible levels by the end of the proliferative phase of healing (15–20 days post-wounding), as observed clinically (Asmussen & Sollner, 1993). Similarly, by this stage the blood vessel density has reached a stable level, which we will regard as average for normal healing.

As with the numerical simulations of Section 4, we have changed three parameters to achieve the keloid and hypertrophic scarring. These were the rate of background nitric oxide production, K, the rate, f_0, at which fibroblasts produce nitric oxide, and finally the responsiveness of fibroblasts to TGF-β; in our simple model this was determined by the initial collagen level, C_0. However, in this more detailed system it appears as the parameter k_{16}, which is the rate at which TGF-β stimulates fibroblast cells to produce collagen. k_{16} has been shown to be higher in hypertrophic scar tissue (Schmid *et al*., 1998). With regard to f_0 and K, we have K higher in keloid scars and f_0 is reduced in hypertrophic lesions (Wang *et al*., 1997).

The hypertrophic pathology shown in Fig. 7(b), and the keloid lesion of Fig. 7(c), both illustrate behaviour and end concentrations matching those results from our earlier model (Section 4). We have the excess collagen and the acellular nature of keloid scars and also the features of hypertrophic lesion, namely a highly cellular scar with the associated spontaneous regression. However, this fuller model captures additional features of these two scar types. As with normal scarring, the final levels of macrophages and TGF-β are negligible, although we also observe that we have increased vasculature relative to the levels shown in Fig. 7(a). The results illustrate nearly a 50% increase in blood vessel density. This is consistent with biological studies which frequently refer to hypertrophic and keloid lesions as highly vascularized (Rockwell *et al*., 1989; Ehrlich *et al*., 1994). It is, however, important to note that despite this increase in blood vessel numbers the hypertrophic and keloid scars are hypoxic, which implies that a large degree of occlusion is occurring. Again, this is supported by numerous studies, in particular the work done by Kischer *et al*. (1982) who specifically focused on this phenomenon.

FIG. 7. Numerical simulations of our full model [eqns (5)–(11)] illustrating normal, hypertrophic and keloid scarring. Column (a) shows the characteristics of normal scarring; in particular we notice a 30% increase in collagen density in comparison to unwounded tissue (~ 100). This corresponds to biological data on scar tissue (Shah *et al*., 1992, 1994; Bardsley *et al*., 1995). The initial conditions used are: $F(0) = F_0 = 100\ \text{cells mm}^{-3}$, $C(0) = C_0 = 0 \times 5.4\ \mu g\, mg^{-1}$ dry weight, $N(0) = N_0 = 1$ nM, $O(0) = O_0 = 0\%$, $M(0) = M_0 = 100\ \text{cells mm}^{-3}$, $T(0) = T_0 = 1 \times 10^{-2}\ \text{ng mm}^{-3}$ and $V(0) = V_0 = 5$. The parameter values used are as follows: $r_1 = 0.92$, $r_2 = 0.5$, $d_1 = 0.12$, $d_2 = 0.000075$, $d_3 = 800$, $d_4 = 3800$, $d_5 = 500$, $d_6 = 20$, $d_7 = 800$, $d_8 = 0.2$, $d_9 = 9.1$, $d_{10} = 0.02$, $k_1 = 0.0004$, $k_2 = 0.006$, $k_3 = 0.5$, $k_4 = 5280$, $k_5 = 4$, $k_6 = 1.2$, $k_7 = 185$, $k_8 = 7$, $k_9 = 0.07$, $k_{10} = 0.015$, $k_{11} = 0.0015$, $k_{12} = 0.01$, $k_{13} = 0.0003$, $k_{14} = 80$, $k_{15} = 12$, $k_{16} = 3.3$, $k_{17} = 2$, $a_1 = 1/300$, $m = 20$, $f_0 = 2.785$, $b_1 = 0.1$ [decay rate of $f(T)$], $K = 0$. These values are discussed further in Appendix A. Column (b) illustrates a hypertrophic lesion. We observe an excess collagen level which gradually regresses to a normal scar. The wound is hypoxic ($O(t) < 10\%$), but is also highly vascularized which implies partial or full blood vessel occlusion, as confirmed by biological data (Kischer *et al*., 1982). The parameters are the same as those used for normal scarring (a) with the exception of $d_4 = 4100$, $f_0 = 0.785$, $k_{16} = 5.4$. Initial conditions also remain the same. Column (c) illustrates keloid scarring. The wound is acellular with high collagen and nitric oxide levels and as with (b) the wound is hypoxic with a high blood vessel density. Parameters and initial conditions are as in (a) except for $d_4 = 4100$, $K = 20\,000$.

6.2. SIMULATION OF ADDITIONAL CLINICAL RESULTS

Clearly, the features we have discussed help support the robustness of our original model, but to further clarify our approach to studying the dynamics of excess scarring we have also been able to generate other clinical observations. In particular, the consequences of inhibiting the NO pathway and the effects of application of the neutralizing antibody to TGF-β (anti-TGF-β) have been considered. To achieve the clinical results numerically, in the case of nitric oxide

inhibition we set the NO density $N(t) = 0$. For the application of anti-TGF-β we have $T(t) = 0$; but in addition we also lower the initial number of macrophages, since the inhibition of the chemoattractant TGF-β would reduce the recruitment of these cells to the wound. For a similar reason, initial fibroblast numbers would also be reduced. The results of the numerical simulations are illustrated in Fig. 8.

Figure 8(b) demonstrates impaired healing associated with the inhibition of wound nitric oxide. As shown by the graph of collagen density, the system takes of the order of 4 months to achieve a level which is even close to that of normal unwounded skin. This result agrees with studies by Schaffer *et al.* (1996), who have shown that *in vivo* inhibition of NO is "parallelled by lowered wound collagen accumulation". In contrast, Fig. 8(c) illustrates improved healing after the application of anti-TGF-β. There are three TGF-β isoforms, each with a slightly different role; however, it is the TGF-β1 isoform we consider here and it is this form of the cytokine to which hypertrophic fibroblasts exhibit increased sensitivity. On the application of the antibody to the TGF-β1 isoform, we observe a cellular wound with fibroblast numbers being close to those of the unwounded dermis (~ 10 cells mm^{-3}). The wound is also less vascularized and the initial deposition of collagen is more gradual than that observed in normal scar formation [Fig. 8(a)], with the final collagen density being lower. All these factors point towards an improved wound healing profile. This behaviour has been observed in numerous experimental studies. For example, Shah *et al.* (1992) injected adult rat wounds with neutralizing antibody to TGF-β and healing occurred without scar tissue. They observed the presence of few macrophages and blood vessels, and collagen levels were reduced. These are all features which are consistent with our numerical simulations. Shah *et al.* (1992) recorded a collagen content in antibody-treated wounds which had an 18% increase compared to the unwounded dermis (~ 100), is agreement with Fig. 8(c); in addition they observed the collagen accumulation to be slower in the treated wounds as we have also shown. Thus, the fact that our model can generate clinically observed results in addition to those relating to excess scarring further supports the robustness of our model. Also, the importance of nitric oxide for collagen accumulation illustrated in Fig. 8(b) helps to support the hypothesis that high levels of NO could account for excess scarring.

7. Discussion

The discovery that mammalian cells synthesize nitric oxide has led to a wide spectrum of studies considering the physiological role of this free radical. One example has been the effects of NO in wound healing. By mathematically modelling the function of nitric oxide in the excess scarring of keloid and hypertrophic lesions, we have been able to gain an insight into a phenomenon which has proven difficult to study biologically and clinically. The numerical simulations of our simple model in Section 4 demonstrated that keloid scarring may be associated with high levels of nitric oxide. We have illustrated that the excess collagen, hypoxia, high vascularity and acellular nature of this type of scarring can be observed as a consequence of increased NO concentration. Hypertrophic lesions have also been characterized by our model; however unlike keloids, the dense cellular scar does not seem to be a consequence of nitric oxide; in fact NO levels tend to be lower. Instead, the fibroblasts from hypertrophic scars have a heightened sensitivity to TGF-β (Schmid *et al.*, 1998), which helps to account for the excess collagen accumulation.

These conclusions from our model are supported by related biological data concerning keloid and hypertrophic scars, although to date, the role of nitric oxide in keloid lesions has not been studied experimentally. It has, however, been extensively observed that the contractile fibroblast, or myofibroblast, is absent in keloids, but present in hypertrophic scars (Ehrlich *et al.*, 1994; Bettinger *et al.*, 1996; Tuan & Nichter, 1998). This property of the scars can be related back to evidence regarding the effects of nitric oxide and TGF-β. Schaffer *et al.* (1997a) noted that the inhibition of NO release resulted in enhanced matrix contraction, which they have suggested is due to NO partially inhibiting the phenotypic change of fibroblast to myofibroblast. In contrast, Desmouliere *et al.* (1993) have

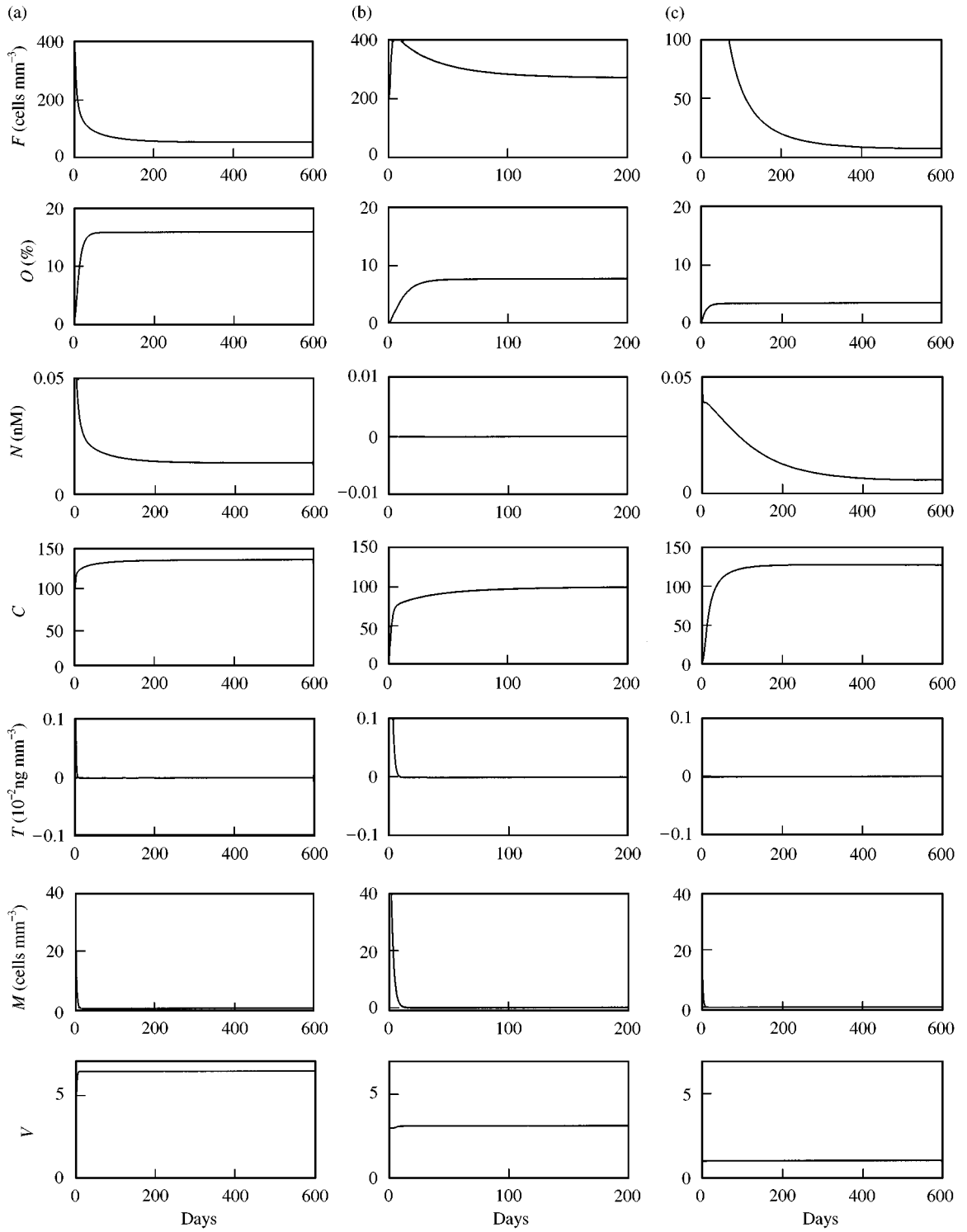

FIG. 8. Numerical simulations of our full model [eqns (5)–(11)] illustrating the consequences of inhibition of the NO pathway and the effects of application of neutralizing antibody to TGF-β. Column (a) acts as reference graphs which demonstrate normal scarring. (Note: The units of collagen density, C are: $\times 5.4\ \mu g\, mg^{-1}$ dry weight). The parameters and initial conditions are as in Fig. 7(a). Column (b) displays the effects of inhibiting nitric oxide. The main feature of its dynamics are impaired healing, with the collagen levels struggling to even reach those of normal dermal tissue (~ 100). The parameters and initial conditions used are as in (a) except we set $N(t) = 0$ to represent to blocking of the nitric oxide pathway. Column (c) is the result of treating a wound with anti-TGF-β. The healing is such that it is less vascularized and the end collagen levels are lower than the normal scar (a), with the collagen accumulation being more gradual. These are all features observed experimentally (Shah *et al.*, 1992). The parameters and initial conditions are as in (a) except we set $T(t) = 0$ to represent the neutralizing of TGF-β and also we have $M(0) = M_0 = 10$ and $F(0) = F_0 = 10$ to represent the effect of reduced levels of their chemoattractant, TGF-β.

demonstrated that TGF-β is a "potent inducer of the myofibroblast phenotype". This suggests a competition between TGF-β and nitric oxide (Ehrlich *et al*., 1994). Therefore, it follows that the extensive presence of contractile fibroblasts in hypertrophic lesions could be associated to the heightened response of hypertrophic fibroblasts to TGF-β and also the reduced synthesis of nitric oxide by these fibroblast cells (Wang *et al*., 1997). In the case of keloid scars, myofibroblasts are absent (Tuan & Nichter, 1998; Ehrlich *et al*., 1994), and given that fibroblasts from these lesions have been shown to produce the same amount of TGF-β as normal fibroblasts (Younai *et al*., 1996) we have a strong hypothesis that a high nitric oxide level is blocking the phenotypic change of fibroblast to myofibroblast. This is reinforced by the observation that contractile fibroblasts are found in normal scar tissue, although to a lesser extent than in hypertrophic lesions (Ehrlich *et al*., 1994). This evidence supports our results obtained from numerical simulations and quasi-steady-state analysis of our model. The notion that nitric oxide may account for keloid scarring can also be related to an observation of Ehrlich *et al*. (1994). They found cultured keloid fibroblasts express the α-smooth muscle actin characteristic of myofibroblasts, despite the fact that *in vivo* they do not. Ehrlich *et al*. (1994) concluded that *in vivo*, local microenvironmental factors must influence and suppress this expression. The microenvironmental factor causing this could be nitric oxide, especially given the other biological characteristics we have discussed.

As well as evidence relating to scar contracture, the role of nitric oxide in excess scarring can be connected to the vascularity of the scars. Both keloids and hypertrophic lesions have been shown to have a high density of microvessels (Rockwell *et al*., 1989; Ehrlich *et al*., 1994), although these are either partially or fully occluded (Kischer *et al*., 1982). Given that a number of studies have indicated that tissue hypoxia could act as a stimulus for angiogenesis (Kischer *et al*., 1975; Rockwell *et al*., 1989; Appleton *et al*., 1996), and since both keloid and hypertrophic scars have been shown to be hypoxic (Kischer *et al*., 1982), this could account for the high degree of vasculature found in these lesions. In terms of blood vessel occlusion, this could be attributed to the stimulation of excess endothelial cell proliferation. As discussed by Fukuo *et al*. (1995) this may be a result of high nitric oxide levels in the case of keloids, and with respect to hypertrophic scars this could be indirectly related to the sensitivity of fibroblasts to TGF-β, a growth factor frequently associated with angiogenesis, albeit indirectly via macrophages (Roberts & Sporn, 1990). Therefore, the hypoxia caused by blood vessel occlusion possibly acts as further stimulation for the observed blood vessel growth. The concept of vasculature in these excess scars is an area we have been able to demonstrate numerically in our full model in Section 6. By simulating this aspect of the scarring pathology it has helped to support the conclusions generated by our simple model.

In addition to our numerical simulations illustrating the features of excess scarring, the characterization of scar types in Section 5, via our model parameter space, could go towards providing a clinical guide to distinguishing between hypertrophic and keloid lesions. This could be beneficial given the current difficulty in categorizing the scars (Blackburn & Cosman, 1966) and the fact that treatment of a supposed hypertrophic lesion could result in reoccurrence if incorrectly diagnosed. So, our model suggests that the rate of nitric oxide production (K, f_0) and the fibroblast sensitivity to TGF-β (k_{16}, C_0) could be key in distinguishing between the lesions.

7.1. THERAPEUTIC IMPLICATIONS

As well as putting forward a method of characterizing scar type, our model hypothesis also leads to a possible suggestion regarding keloid treatment. Currently, reoccurrence of these lesions following treatment such as application of pressure of intralesional administration of triamcinolone is common (Ketchum *et al*., 1974; Nemeth, 1993; Berman & Harlan, 1995), particularly in the case of excision alone. Our model suggests that this is due to the nitric oxide concentration, which we have shown dictates the steady-state levels of the other variables in the system. Thus, we would expect surgical removal of the excess scar to result in the return of collagen to pre-treated levels because the NO

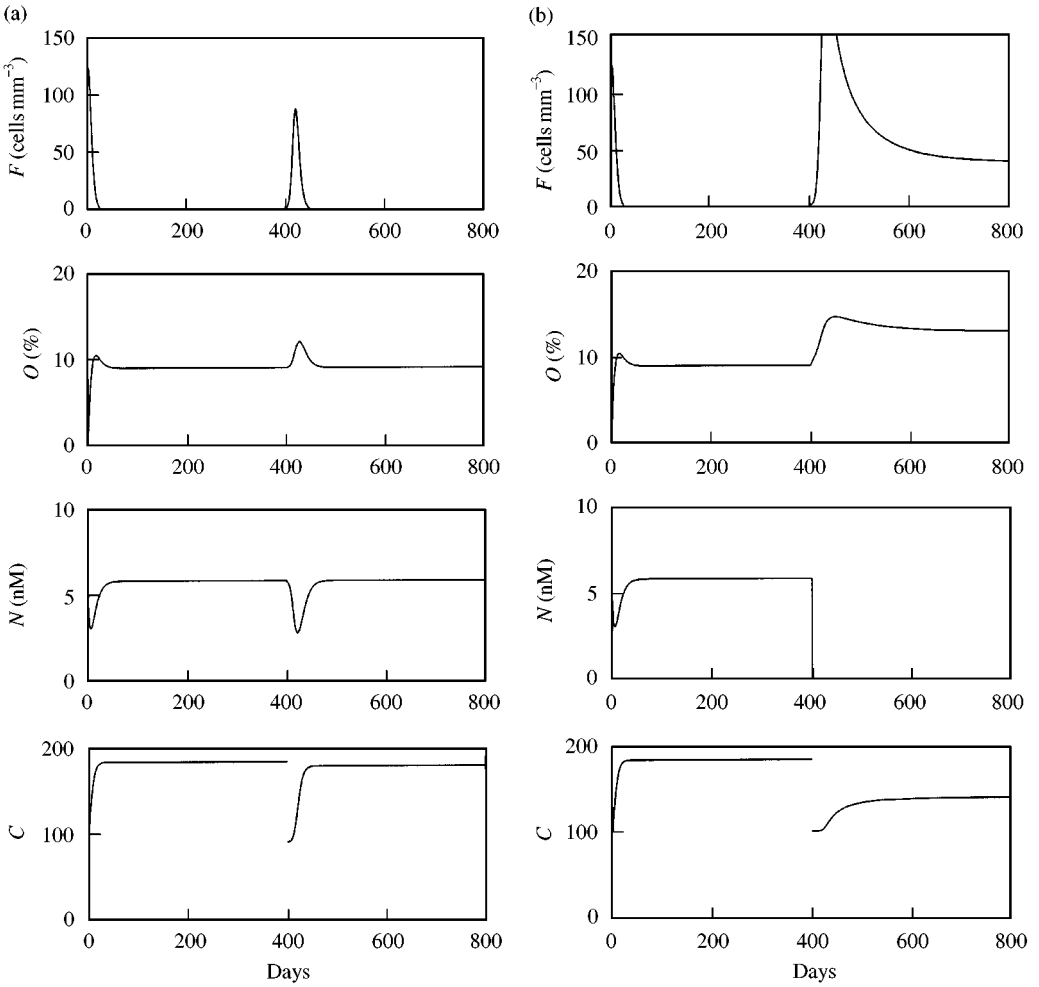

FIG. 9. Numerical simulations using our simple model [eqns (1)–(4)] illustrating the results of two different treatment strategies. Column (a) shows the result of surgical excision of the keloid lesion at day 400 post-wounding. The system was allowed to first evolve to a keloid scar, then at $t = 400$, the fibroblast level was increased to $f(400) = 1$ cell mm^{-3} to represent cell influx following insult, and the collagen density was lowered to 100, which is the density of the unwounded dermis, representing the excision of the scar. The remaining variables and parameters were unchanged. The figure illustrates the reoccurrence of the keloid, with steady-state levels of all the variables returning. The parameter values used are as follows: $r_1 = 0.92$, $d_1 = 0.12$, $d_2 = 0.000075$, $d_3 = 800$, $d_4 = 3800$, $d_5 = 500$, $d_6 = 20$, $d_7 = 800$, $k_1 = 0.0004$, $k_2 = 0.006$, $k_3 = 0.5$, $k_4 = 5280$, $k_5 = 4$, $k_6 = 1.2$, $k_7 = 185$, $v = 7$, $a_1 = 1/300$, $m = 20$, $f_0 = 2.79$, $K = 20\,000$. With initial conditions at $t = 0$ given by $F(0) = F_0 = 100$ cells mm^{-3}, $C(0) = C_0 = 100 \times 5.4\,\mu$g mg^{-1} dry weight, $N(0) = N_0 = 1$ nM and $O(0) = O_0 = 0\%$. (These values are discussed further in Appendix A.) Column (b) shows the effects of surgical excision accompanied by application of a nitric oxide inhibitor, such as L-NMMA. The same process as column (a) was used to model this, with the additional change of lowering the rate of background nitric oxide production, K, to $K = 10$, this models the inhibition of NO. The result of this treatment shows the keloid does not reoccur and a normal scar forms, which is now cellular and less hypoxic. With the exception of the value K, parameters and initial conditions are as in (a).

concentration remains high. So, we suggest that excision would benefit from being accompanied by treatment with an NO inhibitor such as L-NMMA, which could be applied via a cream. We have simulated this approach numerically in Fig. 9(b). We have included an illustration of the consequences of just using excision [Fig. 9(a)], for comparison. Excision is modelled by reducing the collagen levels to that of normal dermal tissue. We would expect such a skin insult to result in cell infiltration, so to mirror this we have introduced a low number of fibroblasts. Finally, the inhibition of nitric oxide is achieved by lowering the background production rate, K.

As shown in Fig. 9(b), when reducing nitric oxide levels in conjunction with surgical excision,

the model predicts that the lesion does not reoccur, but instead evolves to a normal scar. Our parameter space characterization in Section 5 indicates that nitric oxide inhibition alone would not be enough to reduce the scar because this would imply that the initial collagen level, C_0, is greater than C_*, which is the level of collagen at which bifurcation from a cellular to acellular state occurs. The analysis of Section 5 demonstrates that this would give rise to an acellular lesion, characteristic of a keloid, with collagen levels being dictated by C_0; hence we would see no reduction in the scar. Biologically, this role of NO certainly suggests an avenue for further study, particularly given that the hypothesis of high nitric oxide concentration in keloid lesions could be experimentally measured. With regard to hypertrophic scars, our model does not readily lead to a suggestion for treatment, particularly given the frequently observed spontaneous regression associated with these scars (Tuan & Nichter, 1998). However, the possible differentiation of this lesion from that of keloids could certainly be beneficial.

7.2. SOURCE OF BACKGROUND NITRIC OXIDE

With our prediction of high nitric oxide levels accompanying keloid scars, it is necessary to justify this with respect to possible sources of the extra quantities of this free radical. We can explain this by considering one of the major clinical characteristics of this scar, namely that the majority of keloids are found to occur in people with deeply pigmented skin (Peacock *et al*., 1970). Furthermore, the lesions predominantly arise in areas of the body where melanocyte concentration is highest (Rockwell *et al*., 1989); for example, keloids are rarely found on the palms of the hands, where the melanocyte level is minimal (Koohin, 1964). Melanocytes are the cells responsible for the production of the pigmentation chemical, melanin, and they are found in the deep epidermis close to the dermis (Shier *et al*., 1996). The number of these cells does not vary from person to person, but the dispersion of melanin and the amount produced does vary (Shier *et al*., 1996; Koonin, 1964). This is related to nitric oxide, via its involvement in the melanin synthesis pathway.

NO activities tyrosinase, one of the main enzymes responsible for the biosynthesis of melanin (Novellino *et al*., 1998). Thus we would expect to find higher levels of nitric oxide associated with darker skin pigmentation. When a wound occurs, the melanocytes in that region are destroyed, and they are not regenerable (Asmussen & Sollner, 1993), hence the often white appearance of scars. However, keratinocytes, which produce the nitric oxide used in the production of melanin, do regenerate (Romero-Graillet *et al*., 1997). So it would therefore follow that there is more free NO after wounding. Hence, this may be the source of the additional nitric oxide that we hypothesize is present in keloids, particularly given the close proximity of melanocyte cells to the dermis.

Another factor which could explain the enhanced level of nitric oxide arises from the fact that melanin absorbs UV radiation (Sherman & Sherman, 1989). The absence of melanin implies that there would be additional UVA and UVB stimulus for keratinocyte synthesis of NO (Romero-Graillet *et al*., 1997). Relating this back to scar formation would raise the question of why keloids are relatively rare even in people with deeply pigmented skin. This can be answered by noting that this additional free nitric oxide may still result in NO concentrations being kept below the critical level, N_*, we discussed in Section 5. However, if a person was genetically predisposed to produce significant levels of nitric oxide naturally, then the sudden absence of melanocytes taking up this nitric oxide may be sufficient to push the NO concentration beyond N_*, so that the wound heals to give an acellular scar with keloid characteristics. It would also follow that such an effect would be local. This corresponds to data regarding the occurrence of these lesions (Rockwell *et al*., 1989). A suggestion relating to keloid scar prevention arises from this discussion. The skin nitric oxide levels in areas of the body most prone to keloids could be measured, and if found to be too high could be treated with low doses of an NO inhibitor to help prevent keloid formation. This could be an option for people with a known pre-disposition to keloid scars.

The notion that the epidermal cells involved in pigmentation are a source of background nitric oxide, can be related to another characteristic of

keloids, namely the fact that the scar extends beyond the confines of the original wound (Ketchum *et al*., 1974). Production of skin pigment depends on the interaction between melanocytes and neighbouring keratinocytes (Romero-Graillet *et al*., 1996). Not only do keratinocytes produce the nitric oxide involved in the pigmentation reactions, but also melanocytes deposit melanin into the neighbouring keratinocyte cells (Romero-Graillet *et al*., 1997). Given that keratinocytes are closely packed in the epidermis and that nitric oxide is readily diffusible (Lancaster, 1997), it is possible that nitric oxide diffuses beyond the margins of the wound, thus pushing NO levels in that region beyond the critical value. Furthermore, a number of studies have observed a thickened epidermis in keloid lesions (Rockwell *et al*., 1989; Ehrlich *et al*., 1994), thus suggesting the presence of more keratinocytes, which could be related to the fact that nitric oxide can stimulate the proliferation of keratinocytes (Krischel *et al*., 1998). In summary, this discussion suggests that the basal epidermis could certainly be a source of the additional nitric oxide we have described in relation to keloid lesions.

8. Conclusion

The notion that nitric oxide could be involved in excess scar formation has been confirmed by our simple model and the fuller system. The results, coupled with conclusions from existing biological studies on keloid and hypertrophic lesions, is certainly supporting of this hypothesis. A possible extension of this work could be to consider the background nitric oxide production term in more detail, with a view to understanding the mechanism involved in the extension of the lesion beyond the wound margin. In conclusion, our work highlights the potential key role of nitric oxide in keloid scarring and leads us to specific suggestions for possible experimental studies.

CAC was supported by a studentship from the Engineering and Physical Sciences Research Council.

REFERENCES

ADAMS, J. J. (1997). The cell kinetics of murine incisional wound healing. Ph.D. Thesis, University of Manchester.

APPLETON, I., BROWN, N. J. & WILLOUGHBY, D. A. (1996). Apoptosis, necrosis, and proliferation: possible implications in the etiology of keloids. *Am. J. Pathol.* **149,** 1441–1447.

ASMUSSEN, P. D. & SOLLNER, B. (1993). *Wound Care*: *Principles of Wound Healing*. Hamburg: Beiersdorf Medical Bibliothek.

AZZARONE, B., FAILLY-CREPIN, C., DAYA-GROSTEAN, L., CHAPONNIER, C. & GABBIANI, G. (1983). Abnormal behaviour of cultured fibroblasts from nodule and non-affected aponeurosis of Dupuytren's disease. *J. Cell. Physiol.* **117,** 353–361.

BABU, M., DIEGELMANN, R. & OLIVER, N. (1992). Keloid fibroblast exhibit an altered response to TGF-β. *J. Invest. Dermatol.* **99,** 650–655.

BARDSLEY, W. G., SATTAR, A., ARMSTRONG, J. R., SHAH, M., BROSNAN, P. & FERGUSON, M. W. J. (1995). Quantitative analysis of wound healing. *Wound Rep. Reg.* **3,** 426–441.

BASERGA, R. (1976). *Multiplication and division in mammalian cells*: *The Biochemistry of Disease*, vol. 6. New York: Marcel Dekker.

BAUER, E. A. & UITTO, J. (1982). Special tissue collagen: skin. *Collagen in Health and Disease* (Jayson, M. & Weiss, J. eds), pp. 474–487. Edinburgh: Churchill Livingstone.

BERMAN, B. & HARLAN, C. B. (1995). Keloids. *J. Am. Acad. Dermatol.* **33,** 117–123.

BETTINGER, D. A., YAGER, D. R., DIEGELMANN, R. F. & COHEN, I. K. (1996). The effect of TGF-β on keloid fibroblast proliferation and collagen synthesis. *Plast. Reconstr. Surg.* **98,** 827–833.

BLACKBURN, W. R. & COSMAN, B. (1996). Histologic basis of keloid and hypertrophic scar differentiation. *Arch. Pathol.* **82,** 65–71.

CLARK, R. A. F. (1996). Wound repair: overview and general consideration. In: *The Molecular and Cellular Biology of Wound Repair* (Clark R. A. F., ed.), 2nd edn, pp. 3–35. New York: Plenum Press.

COFFEY, R. J. JR., KOST, L. J., LYONS, R. M., MOSES, H. L. & LARUSSO, N. F. (1987). Hepatic processing of transforming growth factor-β in the rat: uptake, metabolism, and biliary excretion. *J. Clin. Invest.* **80,** 750–757.

COLEMAN, C., TUAN, T. L. BUCKLEY, S., ANDERSON, K. D. & WARBURTON, D. (1998). Contractility, transforming growth factor-β, and plasmin in fetal skin fibroblasts: Role in scarless wound healing. *Pediatric Res.* **43,** 403–409.

CROMACK, D. T., SPORN, M. B., ROBERTS, A. B., MERINO, M. J., DART, L. L. & NORTON, J. A. (1987). Transforming growth factor β levels in rat wound chambers. *J. Surg. Res.* **42,** 622–628.

DESMOULIERE, A., GEINOZ, A., GABBIANI, F. & GABBIANI, G. (1993). The transforming growth factor β1 induces α-smooth muscle actin expression in granulation tissue myofibroblasts and in quiescent and growing cultured fibroblasts. *J. Cell Biol.* **122,** 103–111.

EHRLICH, P. H., DESMOULIERE, A., DIEGELMANN, R. F., COHEN, I. K., COMPTON, C. C., GARNER, W. L., KAPANCI, Y. & GABBIANI, G. (1994). Morphological and immunochemical differences between keloid and hypertrophic scar. *Am. J. Pathol.* **145,** 105–113.

FUKUO, K., INOUE, T., MORIMOTO, S., NAKAHASHI, T., YASUDA, O., KITANO, S., SASADA, R. & OGIHARA, T. (1995). Nitric oxide mediates cytotoxicity and basic fibroblast growth factor release in cultured vascular smooth muscle cells. *J. Clin. Invest.* **95,** 669–676.

GHAHARY, A., JUN SHEN, Y., SCOTT, P. G., GONG, Y. & TREDGET, E. E. (1993). Enhanced expression of mRNA for transforming growth factor-β, I and type III procollagen in human post-burn hypertrophic scar tissues. *J. Lab. Clin. Med.* **122,** 465–473.

HASLETT, C. & HENSON, P. (1996). Resolution of inflammation. In: *The Molecular and Cellular Biology of Wound Repair* (Clark, R. A. F. ed.), 2nd edn, pp. 143–168. New York: Plenum Press.

IUVONE, T., CARNUCCIO, R. & DI ROSA, M. (1994). Modulation of granuloma formation by endogeous nitric oxide. *Eur. J. Pharmacol.* **265,** 89–92.

JACKSON, D. S. (1982). Dermal scar. In: *Collagen in Health and Disease* (Jayson, M. & Weiss, J. eds), pp. 466–473. Edinburgh: Churchill Livingstone.

KELLER, E. F. & SEGEL, L. A. (1971). Travelling bands of chemotactic bacteria: a theoretical analysis. *J. theor. Biol.* **30,** 235–248.

KETCHUM, L. D., COHEN, I. K. & MASTERS, F. W. (1974). Hypertrophic scars and keloids: a collective review. *Plast. Reconstr. Surg.* **53,** 140–154.

KIRK, S. J., REGAN, M. C., PALMER, R. M. J., MONCADA, S., WASSERKRUG, H. L., BARBUL, A. (1993). The role of nitric oxide in wound collagen deposition. *Surg. Forum* **44,** 706–708.

KISCHER, C. W., SHETTER, M. R. & SHETLAR, C. L. (1975). Alterations of hypertrophic scars induced by mechanical pressure. *Arch. Dermatol.* **111**, 60.

KISCHER, C. W., THIES, A. C. & CHVAPIL, M. (1982). Perivascular myofibroblasts and microvascular occlusion in hypertrophic scars and keloids. *Hum. Pathol.* **13,** 819–824.

KNIGHTON, D. R., SILVER, I. A. & HUNT, T. K. (1981). Regulation of wound-healing angiogenesis—Effect of oxygen gradients and inspired oxygen concentration. *Surgery* **90,** 262–269.

KNIGHTON, D. R., HUNT, T. K., SCHEUENSTUHL, H., HALLIDAY, B. J., WERB, Z. & BANDA, M. J. (1983). Oxygen tension regulates the expression of angiogenesis factor by macrophages. *Science* **221,** 1283–1285.

KNIGHTON, D. R. & FIEGEL, V. D. (1989). Macrophage-derived growth factors in wound healing: regulation of growth factor production by the oxygen microenvironment. *Am. Rev. Respir. Dis.* **140,** 1108–1111.

KOONIN, A. J. (1964). The aetiology of keloids: a review of the literature and a new hypothesis. *S. Afr. Med. J.* **38,** 913–916.

KRISCHEL, V., BRUCH-GERHARZ, D., SUSCHER, C., KRONCKE, K., RUZICKA, T. & KOLB-BACHOFEN, V. (1998). Biphasic effect of exogenous nitric oxide on proliferation and differentiation in skin derived keratinocytes but not fibroblasts. *J. Invest. Dermatol.* **111,** 286–291.

KU, D. D. (1996). Nitric oxide- and nitric oxide donar-induced relaxation. *Meth. Enzymol.* **269,** 107–119.

LANCASTER, J. R. JR. (1997). A tutorial on the diffusibility and reactivity of free nitric oxide. *Nitric Oxide*: *Biol. Chem.* **1,** 18–30.

LIU, B. & CONNOLLY, M. K. (1998). The pathogenesis of cutaneous fibrosis. *Sem. Cutaneous Med. Surg.* **17,** 3–11.

LEIBOVICH, S. J. & ROSS, R. (1975). The role of the macrophage in wound repair. *Am. J. Pathol.* **78,** 71–91.

LISIDS, J., HOYLE, C. H. V. & BEONSTOCH, G. (1997). Nitric oxide: introduction and historical background. In: *Nitric Oxide in Health and Disease* (Lisids, J., Hoyle, C. H. V. & Beonstoch, G., eds), pp. 3–11. Cambridge: CUP.

MCCALLION, R. L. & FERGUSON, M. W. J. (1996). Fetal wound healing and the development of antiscarring therapies for adult wound healing. In: *The Molecular and Cellular Biology of Wound Repair* (Clark, R. A. F., ed.), 2nd edn, pp. 561–591. New York: Plenum Press.

MORGAN, C. J. & PLEDGER, W. J. (1992). Fibroblast proliferation. In: *Wound Healing*: *Biochemical and Clinical Aspects* (Cohen, I. K., Piegelmann, R. F. & Linblad, W. J., eds), pp. 63–76. Philadelphia: W. B. Saunders Co.

MURRAY, J. C. & PINNELL, S. R. (1992). Keloids and excessive dermal scarring. In: *Wound Healing*: *Biochemical and Clinical Aspects* (Cohen, I. K., Piegelmann, R. F. & Linblad, W. J., eds), pp. 500–509. Philadelphia: W. B. Saunders Co.

NEMETH, A. J. (1993). Keloids and hypertrophic scars. *J. Dermatol. Surg. Oncol.* **19,** 738–746.

NIINIKOSKI, J., HEUGHAN, C. & HUNT, T. K. (1971). Oxygen and carbon dioxide tensions in experimental woounds. *Surg. Gynecol. Obstet.* **133**, 1003–1007.

NISSEN, N. N., POVERINI, P. J., KOCH, A. E., VOLIN, M. V., GAMELLI, R. L. & DIPIETRO, L. A. (1998). Vascular endothelial growth factor mediates angiogenic activity during the proliferative phase of wound healing. *Am. J. Pathol.* **152,** 1445–1452.

NODDER, S. & MARTIN, P. (1997). Wound healing in embryos: a review. *Anat. Embryol.* **195,** 215–228.

NOVELLINO, L., D'ISCHIA, M. & PROTA, G. (1998). Nitric oxide-induced oxidation of 5,6-dihydroxyindole and 5,6-dihydroxyindole-2-carboxylic acid under aerobic conditions: non-enzymatic route to melanin pigments of potential relevance to skin (photo)protection. *Biochim. Biophys. Acta* **1425,** 27–35.

OLSEN, L., SHERRATT, J. A. & MAINI, P. K. (1995). A mechanochemical model for adult dermal wound contraction and the permanence of the contracted tissue displacement profile. *J. theor. Biol.* **177,** 113–128.

OVERALL, C. M., WRANA, J. L. & SODECK, J. (1989). Independent regulation of collagenase, 72-kDa progelatinase, and metalloendoproteinase inhibitor expression in human fibroblasts by transforming growth factor-β. *J. Biol. Chem.* **264,** 1860–1869.

PEACOCK, E. E. JR., MADDEN, J. W. & TRIER, W. C. (1970). Biologic basis of treatment of keloid and hypertrophic scars. *South Med. J.* **63,** 755–760.

PETTET, G., CHAPLAIN, M. A. J., MCELWAIN, D. L. S. & BYRNE, H. M. (1996). On the role of angiogenesis in wound healing. *Proc. Roy. Soc. London B* **263,** 1487–1493.

POSTLETHWAITE, A. E., KESKI-OJA, J., MOSES, H. L. & KANG, A. H. (1987). Stimulation of the chemotactic migration of human fibroblasts by transforming growth factor β. *J. Exp. Med.* **165,** 251–256.

RICHES, D. W. H. (1996). Macrophage involvement in wound repair, remodelling and fibrosis. In: *Molecular and Cellular Biology of Wound Repair* (Clark, R. A. F., ed.), 2nd edn, pp. 95–131. New York: Plenum Press.

ROBERTS, A. B., SPORN, M. B., ASSOIAN, R. K., SMITH, J. M., ROCHE, N. S., WAKEFIELD, L. M., HELNE, U. I., LIOTTA, L. A., FALANGA, V., HEHRL, J. H. & FAUCI, A. S. (1986). Transforming growth factor type β: rapid induction of fibrosis and angiogenesis *in vivo* and stimulation of collagen formation *in vitro*. *Proc. Nat. Acad. Sci. U.S.A.* **83,** 4167–4171.

ROBERTS, A. B. & SPORN, M. B. (1990). The transforming growth factor-β's. In: *Peptide Growth Factors and Their Receptors*: *Handbook of Experimental Pharmacology* (Sporn, M. B. & Roberts, A. B., eds), vol. 1, pp. 417–472. Berlin: Springer-Verlag.

ROBERTS, A. B. & SPORN, M. B. (1996). Transforming growth factor-β. In: *The Molecular and Cellular Biology of Wound Repair* (Clark, R. A. F., ed.), 2nd edn, pp. 275–308. New York: Plenum Press.

ROCKWELL, W. B., COHEN, I. K. & EHRLICH, H. P. (1989). Keloids and hypertrophic scars: a comprehensive review. *J. Plast. Reconstr. Surg.* **84,** 827–837.

ROMERO-GRAILLET, C., ABERDAM, E., BIAGOLI, N., MASSABNI, W., ORTONNE, J. & BALLOTTI, R. (1996). Ultraviolet B radiation acts through the nitric oxide and cGMP signal transduction pathway to stimulate melanogeneis in human melanocytes. *J. Biochem. Chem.* **271,** 28052–28056.

ROMERO-GRAILLET, C., ABERDAM, E., CLEMENT, M., ORTONNE, J. & BALLOTTI, R. (1997). Nitric oxide produced by ultraviolet-irradiated keratinocytes stimulates melanogenesis. *J. Clin. Invest.* **99,** 635–642.

RUSSELL, J. D. & WITT, W. S. (1976). Cell size and growth characteristics of cultured fibroblasts isolated from normal and keloid tissue. *Plast. Reconstr. Surg.* **57,** 207–212.

SARIH, M., SOUVANNAVONG, V. & ADAM, A. (1993). Nitric oxide synthase induces macrophage death by apoptosis. *Biochem. Biophys. Res. Commun.* **191,** 501–508.

SCHAFFER, M. R., TANTRY, U., GROSS, S. S., WASSERKRUG, H. L. & BARBUL, A. (1996). Nitric oxide regulates wound healing. *J. Surg. Res.* **63,** 237–240.

SCHAFFER, M. R., EFRON, P. A., THORNTON, F. J., KLINGEL, K., GROSS, S. S. & BARBUL, A. (1997a). Nitric oxide, an autocrine regulator of wound fibroblast synthetic function. *J. Immun.* **158,** 2375–2381.

SCHAFFER, M. R., TANTRY, U., VAN WESEP, R. A. & BARBUL, A. (1997b). NO metabolism in wounds. *J. Surg. Res.* **71,** 25–31.

SCHMID, P., ITIN, P., CHERRY, G., BI, C. & COX, A. (1998). Enhanced expression of transforming growth factor-β type I and type II receptors in wound granulation tissue and hypertrophic scar. *Am. J. Pathol.* **152,** 485–493.

SHAH, M., FOREMAN, D. M. & FERGUSON, M. W. J. (1992). Control of scarring in adult wounds by neutralising antibody to transforming growth factor β. *Lancet* **339,** 213–214.

SHAH, M., FOREMAN, D. M. & FERGUSON, M. W. J. (1994). Neutralising antibody to TGF-$\beta_{1,2}$ reduces cutaneous scarring in adult rodents. *J. Cell Sci.* **107,** 1137–1157.

SHERMAN, I. W. & SHERMAN, V. G. (1989). *Biology*: *A Human Approach*, 4th edn. New York: OUP.

SHIER, D., BUTLER, J. & LEWIS, R. (1996). *Hole's Human Anatomy and Physiology*, 7th Edn. Dubuque IA: WCB.

SULLIVAN, K. M., LORENZ, P., MEULI, M., LIN, R. Y. & ADZICK, S. N. (1995). A model of scarless human fetal wound repair is deficient in transforming growth factor beta. *J. Pediatr. Surg.* **30,** 198–203.

TUAN, T. & NICHTER, L. S. (1998). The molecular basis of keloid and hypertrophic scar formation. *Mol. Med. Today* **4,** 19–24.

UITTO, J. (1986). Interstitial collagens. In: *Biology of the Integument* 2: *Vertebrates* (Bereiter-Hahn, J., Matoltsy, A. G. & Richards, K. S., eds), pp. 800–809. Berlin: Springer-Verlag.

WAHL, S. M., HUNT, D. A., WAKEFIELD, L. M., MCCARTNEY-FRANCIS, N., WAHL, L. M., ROBERTS, A. B. & SPORN,, M. B. (1987). Transforming growth factor type β induces monocyte chemotaxis and growth factor production. *Proc. Nat. Acad. Sci. U.S.A.* **84**, 5788–5792.

WAKEFIELD, L. M., WINOKUR, T. S., HOLLANDS, R. S., CHRISTOPHERSON, K., LEVINSON, A. D. & SPORN, M. B. (1990). Recombinant latent transforming growth factor β1 has a longer plasma half-life in rats than active transforming growth factor β1, and a different tissue distribution. *J. Clin. Invest.* **86,** 1976–1984.

WANG, R., GHAHARY, A., SHEN, J. S., SCOTT, P. G. & TREDGET, E. (1997). Nitric oxide synthase expression and nitric oxide production are reduced in hypertrophic scar tissue and fibroblasts. *J. Invest. Dermatol.* **108,** 438–444.

WELLER, R., SHERRATT, J., MCKENZIE, R. & HUNTER, J. (2000). Blood flow in psoriatic plaques is determined by nitric oxide production (submitted).

WINK, D. A., GRISHAM, M. B., MITCHELL, J. B. & FORD, P. C. (1996). Direct and indirect effects of nitric oxide in chemical reactions relative to biology. *Meth. Enzymol.* **268,** 12–31.

WITTE, M. B., SCHAEFFER, M. R. & BARBUL, A. (1996). Phenotypic induction of nitric oxide is critical for synthetic function in wound fibroblasts. *Surg. Forum* **47,** 703–705.

YOUNAI, S., VENTER, G., VU, S., NICHTER, L., NIMNI, M. E. & TUAN, T. (1996). Role of growth factors in scar contraction. An *in vitro* analysis. *Ann. Plast. Surg.* **36,** 495–501.

APPENDIX A

Parameter Estimates

We have been able to find biological data for most of the parameters in our simple model; however, given the large number of parameters in the extended model, obtaining so many values has proven to be more difficult. In such cases, we have attempted to make order of magnitude estimates where possible.

A.1. SIMPLE MODEL PARAMETERS

So we begin by establishing the concentrations and densities of normal unwounded skin for the variables in our simple model.

- F_0: Human fibroblasts have a cell volume of approximately $3400\,\mu m^3$ (Russell & Witt, 1976) and are found to be sparsely distributed in the dermis (Morgan & Pledger, 1992). This coincides with a cell density used in experiments of the order of $10^4\,\text{cells}\,\text{ml}^{-1}$ (Wahl *et al.*, 1987). Hence, the density of fibroblasts in unwounded skin is taken as: $F_0 = 10\,\text{cells}\,\text{mm}^{-3}$.
- C_0: Data from Shah *et al.* (1994) gives a collagen content in normal skin of $536\,\mu\text{g}\,\text{mg}^{-1}$

dry weight. For convenience, we scale this to 100 for normal skin ($C_0 = 100$) and we can use data by Shah *et al.* (1992) to obtain a measure of collagen levels in normal scar tissue. They recorded a final collagen density in scar tissue of 690 $\mu g\,ml^{-1}$ dry weight, which yields a 29% $[= 100 \times (690 - 536)/536]$ increase in collagen. This provides an indication of what level we would expect our model of normal healing to produce.

The remaining parameters for the basic model are discussed below:

r_1, k_1, d_1: Fibroblast cells are known to have a cell cycle time of approximately 18 hr (Morgan & Pledger, 1992), at the end of which we have population doubling via mitotic division. Thus the growth rate, $r_1 = \ln 2/0.75 = 0.924\,day^{-1}$. Related to this is the death rate of fibroblasts, d_1. The cells have been demonstrated to have a lifespan of the order of 16 population doublings (based on the data using human age and sex-matched cell lines) (Azzarone *et al.*, 1983). Thus, it follows that the half-life of human fibroblasts is $T_{1/2} = 8 \times 0.75 = 6$ days. This then yields a death rate of $d_1 = \ln 2/T_{1/2} = 0.116\,day^{-1}$.

The maximal fibroblast density, k_1, has been studied in a number of papers (Azzarone *et al.*, 1983; Overall *et al.*, 1989). Cells grown to confluence in culture displayed a final density of approximately 2×10^4 cells cm^{-2} (Azzarone *et al.*, 1983), where the cells are grown in a monolayer. Thus, it follows that this is equivalent to $\sim 3 \times 10^6$ cells $cm^{-3} = 3 \times 10^3$ cells mm^{-3}. Hence, a value of $k_1 \approx 0.0004$ is consistent with experimental results.

k_2: There is an absence of experimental evidence describing the effect of collagen density on fibroblast growth. Therefore to determine k_2 we use the fibroblast equation (1), which has steady state, F_s, C_s, given by $r_1(1 - F_s k_1 - C_s k_2) - d_1 = 0$. (Note: We ignore the effects of oxygen on the decay rate, d_1, because there would be no hypoxic effects in the unwounded dermis.) We would expect the unwounded dermal levels $F_s = F_0$, $C_s = C_0$, to be an equilibrium, and thus knowing r_1, k_1 and d_1 enables us to determine an approximate value for k_2. This gives $k_2 = (1 - F_0 k_1 - d_1/r_1)/C_0 \approx 0.008$. Since phenotypic cell characteristics during wounding are altered our model does not actually exhibit an unwounded steady state, also given that scars are frequently as cellular as unwounded tissue, we would expect collagen to have a slightly lower effect on fibroblast numbers than the above value of k_2 suggests. So instead we use this value of k_2 as a guide to order of magnitude, and we will take k_2 to be slightly smaller, with $k_2 \approx 0.006$.

$q(O) = (p(1 + k_3) + O)/(p + O)$: Niinikoski *et al.* (1971) report that actively dividing fibroblasts can be detected in regions where oxygen tension is greater than 15 mmHg ($\sim 2\%$). This yields $p = 2$ in our function. The strength of the effect of oxygen on fibroblast proliferation is reflected by the parameter k_3. We would expect to see virtually no proliferation at $\sim 0\%$ oxygen, and thus if we consider the basic form of our fibroblast equation we would expect $dF/dt = r_1 F(1 - k_1 F) - (d_1 + k_3)F \approx -d_1 F$. Hence, we would predict k_3 to be of a similar order of magnitude to r_1, so that $k_3 \approx 0.5$ would be a reasonable estimate.

d_2: Uitto (1986) determined the half-life of collagen turnover in the adult dermis to be 2.5 yr. This yields a decay rate of $d_2 = \ln 2/(365 \times 2.5 \times F_0) = 7.6 \times 10^{-5}\,cell^{-1}\,day^{-1}$, where $F_0 = 10$ cells mm^{-3} in the normal unwounded dermis.

d_3, d_4: Given the difficulty in finding exact data on the half-life of oxygen in skin tissue, we have estimated it using data on its diffusivity. Oxygen diffuses at a rate of $5 \times 10^{-2}\,cm^2\,hr^{-1}$ (Keller & Segel, 1971) ($\sim 1389\,\mu m^2\,s^{-1}$). A study by Knighton & Fiegel (1989) remarks that "oxygen is rapidly consumed as it diffuses from the capillary" and an estimate of the range of this movement is of the order of 220 μm in the wounded dermis. (In normal dermis the range of movement is of the order of 300 μm). Thus, the Einstein–Smoluchowski equation (Lancaster, 1997)

$$\langle \Delta x \rangle^2 = 2Dt$$

where D is the diffusion coefficient, t is time and Δx is the average distance allows us to estimate the half-life of oxygen. So we have $(220)^2 = 2 \times 1389 \times t$; thus $t_{1/2} \sim 17.4$ s. This half-life is a result of the combined effects of the oxygen decay terms. The wide range of possible targets for oxygen implies that it is likely that the general

decay term will dominate over the reaction with nitric oxide. Also given that in normal tissue there would be no nitric oxide synthesized from fibroblasts or macrophages (Schaffer *et al*., 1979) it follows that $d_4 \approx 3800\,\text{day}^{-1}$ (i.e. half-life of $\sim$18 s). When nitric oxide is present we would expect the reaction to be quite rapid. A rate constant for such a reaction has been calculated to be about $9 \times 10^6\ \text{M}^{-1}\,\text{s}^{-1}$ (Wink *et al*., 1996); the reaction was carried out at a range of pH and temperatures and the rate constant did not vary, so this is a reasonable estimate for the parameter. In the units used in our model this yields a value of $d_3 \approx 80\,\text{nM}^{-1}\,\text{day}^{-1}$.

d_5, d_6, d_7, k_7: Nitric oxide has been recorded to have an *in vivo* half-life of the order of 5–15 s (Lancaster, 1997), hence we would expect the combined effects of the nitric oxide decay terms to give a half-life of this order of magnitude. There is an absence of specific experimental data so given the high reactivity of nitric oxide with oxygen and haemoglobin we would expect these to be the principal sources of decay. As estimate for the general decay term d_5N would be of the order of seconds given the extensive interaction of nitric oxide with extracellular components of the dermis. A half-life as high as 50 s has been observed for nitric oxide and since one of the principal reactions which leads to such a half-life is between the free radical and oxygen, we conclude that an estimate of 120 s for the half-life of nitric oxide in the absence of oxygen is not unreasonable. So in the absence of further information we take, $d_5 = (\ln 2/120)\text{s}^{-1} \approx 500\ \text{day}^{-1}$. To estimate the reaction rate of nitric oxide and oxygen the lack of experimental data forces us to make approximations. We assume the half-life of nitric oxide (5 s) is a consequence of the reaction with oxygen and the general decay term, thus giving $d_5 + d_7O = \ln 2/120 + d_7O = \ln 2/5\ \text{s}^{-1}$. Hence, $d_7O = \ln 2(115/600)\text{s}^{-1} \approx 11500\ \text{day}^{-1}$. Assuming such a reaction occurs in the wound environment where oxygen levels are not optimal, we take $O = 15\%$, which yields $d_7 \approx 800$.

We would expect the removal of NO through the paracrine reaction with fibroblast cells to be significantly lower compared with extracellular reactions. The reasoning for this is partially related to the distance between cells which nitric oxide would have to cover for a reaction to take place. Therefore, we would expect the reaction of nitric oxide with fibroblasts to be of the order of minutes, i.e. $d_6F \approx 200\,\text{day}^{-1}$. By assuming an average density of fibroblasts, we take $d_6 \approx 20$.

Finally we approximate the removal of nitric oxide via the reaction with haemoglobin in the blood vessels. This is particularly difficult to estimate because *in vitro* data on the association rate of NO with haemoglobin gives a value of about 0.1 s. This is a very rapid rate and contradicts the existence of the reaction of nitric oxide with endothelial cells with causes blood vessel dilation. So a possible explanation for a slower haemoglobin reaction rate would be that a substantial amount of the haemoglobin is already bound. Such an argument has been put forward in several studies (Lancaster 1997; Weller *et al*., unpublished data). Thus, based on this hypothesis we estimate the reaction rate to be of a similar order to that of NO with oxyhaemoglobin which is $1.5 \times 10^7\ \text{M}^{-1}\,\text{s}^{-1}$ (Wink *et al*., 1996). This yields $k_7V \approx 1296\,\text{nM}^{-1}\,\text{s}^{-1}$. Assuming an average vascular density yields $k_7 \approx 185$.

Despite the numerous assumptions we have applied in approximating these decay rates, the important feature is that nitric oxide undergoes a rapid turnover which results in the free radical rapidly attaining its steady-state level and it is this feature which has been our main interest in studying the biological system.

k_4: Due to the absence of experimental data on the rate of oxygen production by the vasculature, together with the fact that $V(t)$ is a notional variable in our model, leads us to approximate k_4 by considering the oxygen steady state of unwounded tissue, which is $O_0 = 20\%$ (Knighton *et al*., 1983). The oxygen differential equation (10) yields, $\text{d}O/\text{d}t = k_4V - dO$. We have an estimate for d, the half-life of oxygen in normal tissue, and by assuming normal skin has average vasculature ($V = 6$), we have $0 = k_4 \times 6 - 1848 \times 20$, hence, $k_4 \approx 5280$.

$s(N) = k_5N/(N + k_6)$: This function models dilation of blood vessels relative to those from unwounded skin. Experimental data by Ku (1996) suggest this saturating functional form for $s(N)$. Ku (1996) carried out experiments under different oxygen concentrations and observed that the value of k_6 decreases with oxygen percentage. Ku (1996) gives $k_6 \approx 1.6\,\text{nM}$ for 20% oxygenation, which is equivalent to normal

skin tissue. Given that wounds are hypoxic, $k_6 \approx 12$ nM would be a reasonable order of magnitude estimate.

Finally, we estimate k_5 which models the strength of the effect of nitric oxide on dilation. Given that Ku (1996) recorded a dilated blood vessel diameter of ~ 1.5 mm and a relaxed diameter of ~ 0.35 mm leads us to take a dilation factor of $k_5 = 1.5/0.35 = 4$. This seems reasonable given the notional nature of the vasculature in our model.

v: Assuming, as with $V(t)$, that the density of patent vasculature is measured on a scale of 0–10, with 0 representing virtually no patent vasculature and 10 corresponding to a high density of non-occluded blood vessels. Given that keloids and hypertrophic scars have been widely described as having a vasculature which is predominantly partially or fully occluded (Rockwell *et al.*, 1989), we take $v \approx 1$. For normal scar tissue there is a average amount of vascularity with blood vessels generally patent, so $v \approx 7$.

f_0: Wang *et al.* (1997) carried out a human study, where they measured the level of nitric oxide produced by wound fibroblasts from normal hypertrophic scar tissue. This gave a mean value of $f_0 \approx 1.55$ for hypertrophic cells (although there was significant variation in this value between patients) and $f_0 \approx 2.8$ for normal fibroblasts. The value for normal scar tissue is supported by a study by Schaffer *et al.* (1997a) which demonstrates that wound fibroblasts spontaneously synthesize and release nitric oxide at a rate of ~ 4.60 nmol μg^{-1} DNA/48 hr. Information on mammalian cells reveals that a cell has approximately 10^{-2} g of DNA per cell (Baserga, 1976). Using this gives an NO production rate of $\sim 2.3 \times 10^{-6}$ nmol cell^{-1} day^{-1}, which leads to a value of $f_0 \approx 2.3$. For the purposes of our simulations we take the value for f_0 from the data by Wang *et al.* (1997) due to possible error in the approximation regarding cell DNA content used in obtaining a value from the results of Schaffer *et al.* (1997a).

A.2. SENSITIVITY ANALYSIS OF THE SIMPLE MODEL PARAMETERS

Having fixed many of the parameters in this simple model using experimental data, to confirm our values we also carried out a parameter sensitivity analysis. The measure of sensitivity, S, is the percent change in solution measure (which we take collagen steady-state density) divided by percentage change in parameter. Therefore, a value of $S = \pm 1$ reflects a change in output magnitude in equal proportion to the change in input. As we can see from Fig. A1, the solution is highly robust to changes in both parameter values and initial conditions.

A.3. EXTENDED MODEL PARAMETERS

As a result of the added complexity of the extended model we have found it difficult to find specific data on a number of parameters. As a consequence, the values which we will now go on to discuss are not as concrete as those of the simple model, but provide order of magnitude approximations which are still a useful guide. Below we begin by explaining the initial concentrations of the additional variables in our full model.

M_0: Leibovich & Ross (1975) observed a maximum number of ~ 200 macrophages mm^{-3} in wound-healing experiments carried out on guinea pigs. Similar values were found by Wahl *et al.* (1987). Therefore, given that macrophages reach a maximal level at 3 days post-wounding (Leibovich & Ross, 1975) (at time $t = 0$ days in the full model), $M_0 = M(0) = 100$ cells mm^{-3} is a reasonable order of magnitude estimate.

V_0: Vasculature, $V(t)$, is a notional parameter in our model which ranges from 0 to 10, with 0 being avascular and 10 being highly vascularized. It is reasonable to assume that there is a moderate level of blood vessels by 3 days post-wounding ($t = 0$), and we take $V_0 = V(0) = 5$. However, this numerical value is inevitably arbitrary since the variable is notional.

T_0: We are unaware of specific data on the TGF-β concentration during wounding healing; however, studies by Cromack *et al.* (1987) demonstrated that TGF-β levels are at a peak during fibroblast proliferation and collagen synthesis. So to estimate an initial concentration at 3 days post-wounding we take the level used in experiments which resulted in maximal cell proliferation and collagen synthesis. This value was

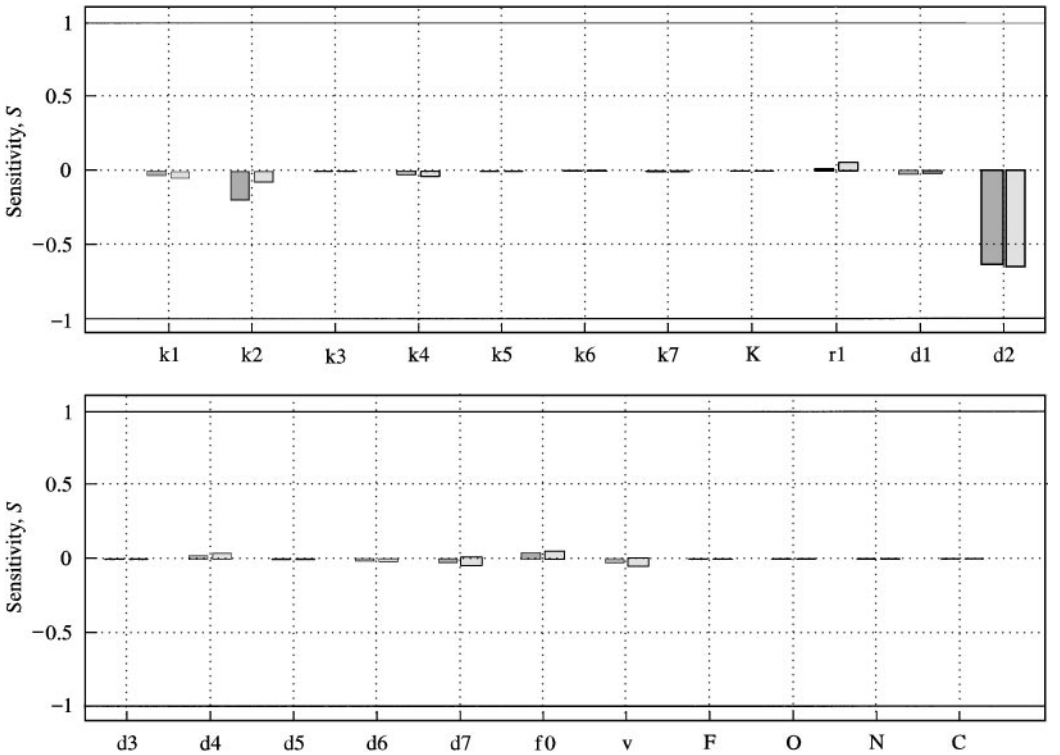

FIG. A1. Bar chart displaying the results of a parameter sensitivity analysis. We varied each parameter and initial condition by $\pm$ 50% from our fixed set of parameter values which are as follows: $r_1 = 0.92$, $d_1 = 0.12$, $d_2 = 0.000075$, $d_3 = 800$, $d_4 = 3800$, $d_5 = 500$, $d_6 = 20$, $d_7 = 800$, $k_1 = 0.0004$, $k_2 = 0.006$, $k_3 = 0.5$, $k_4 = 5280$, $k_5 = 4$, $k_6 = 1.2$, $k_7 = 185$, $v = 7$, $a_1 = 1/300$, $m = 20$, $f_0 = 2.79$, $K = 0$. With, initial conditions at $t = 0$ given by $F(0) = F_0 = 100\,\text{cells}\,\text{mm}^{-3}$, $C(0) = C_0 = 100 \times 5.4\,\mu\text{g}\,\text{mg}^{-1}$ dry weight, $N(0) = N_0 = 1$ nM and $O(0) = O_0 = 0\%$. (These values are discussed further in this section.) The sensitivity measure, S, is the percent change in solution measure (collagen steady-state density, C_s) divided by the percent change in parameter. So on our chart $\pm$ 1 reflects a change in output which is in equal proportion to the change in input. Given that all results are bounded by $\pm$ 1 it demonstrates that the parameters for the simple model are highly robust and supports our choice of values: (■) + 50%; (□) − 50%.

$10\,\text{ng}\,\text{ml}^{-1}$ (Wahl *et al.*, 1987; Roberts *et al.*, 1986) which yields $T_0 = 1$.

Finally, we discuss the extra parameters which appear in our fuller model:

r_2: Wounds treated with anti-TGF-β, like normal scars, are cellular and healing still occurs (Shah *et al.*, 1992). This suggests that $r_1 > r_2 T$. Because TGF-β indirectly stimulates fibroblast proliferation it is difficult to find accurate data on the rate r_2, so that our only guide is $r_2 < r_1/T = 0.9/1$. We take $r_2 = 0.5$.

k_9, k_{10}: A study by Sullivan *et al.* (1995) reports that "macrophages are the principal source of TGF-β in adult wounds". From this we can deduce that $k_9 > k_{10}$, i.e. the rate of macrophage production of TGF-β is greater than that of fibroblasts. A similar relation holds for nitric oxide where the difference in rates was a factor of 4.5 (Schaffer *et al.*, 1997a), and in the absence of other information we estimate the same factor for TGF-β production rates, which gives $k_{10} \times 4.5 \approx k_9$.

Because macrophages are at a maximum at 3 days post-wounding (Leibovich & Ross, 1975), it follows that it is likely that TGF-β concentration is also close to its maximum at this point, hence we would expect decay to dominate. Given that decay occurs with a half-life of at most 100 min, we may predict the production rate to be slower. Thus, $k_9 M < ((\ln 2)/100)\,\text{min}^{-1} \approx 10\,\text{day}^{-1}$, so as $M_0 = 100$ and in the absence of further data we take $k_9 \approx 0.07$ and thus $k_{10} \approx 0.015$.

k_{11}: Obtaining exact biological data on the rate of neovascularization is very difficult, especially given that blood vessel density is a notional parameter in our model. However, experimental

results by Knighton *et al.* (1981) enable us to make an approximate order of magnitude estimate of the k_{11} parameter. They measured blood vessel growth in rabbit ear chambers and recorded their results as a percentage of the chamber filled at each day after the initial vessel implantation. Results from the experiments carried out in 20% oxygen gives a vasculature growth rate of about 6.7% per day. If we relate this to the form of our differential equation for $V(t)$ [eqn (7)], we have $\mathrm{d}V/\mathrm{d}t \approx k_{11}V_eM_e = 0.67$. (Note: We would not expect to see crowding affecting the growth rate in the experiment and oxygen concentration was consistently kept at the level of normal tissue so no effects due to hypoxia would have been observed, hence we ignored these components of our differential equation.) If we assume V_e is an average level of vasculature and macrophage numbers, M_e, are such that they are at a level which would provide sufficient angiogenic factors, as would be the case in the experiment, we obtain $\mathrm{d}V/\mathrm{d}t \approx k_{11} \times 5 \times 100 = 0.67$, which yields a value of $k_{11} \sim 0.0015$.

k_{12}: The graphs and results from the rabbit ear chamber experiments by Knighton *et al.* (1981) suggest that crowding effects due to blood vessel density only play a role in angiogenesis when a very high percentage of the ear chamber is filled with blood vessels. Given that we have defined V to vary between 0 and 10, we assume that $V = 10 \equiv$ a high density of occluded blood vessels, has begun to cause crowding. Thus, given that V is a generic variable and we have no exact data we choose $k_{12} \approx 0.01$ as an order of magnitude estimate.

k_{13}: We would expect the effect of collagen density on blood vessel proliferation to be less than its effect on fibroblast cell density because in the example of the high collagen density keloid lesions an acellular, highly vascularized environment is observed. Thus it follows that $k_{13} < k_2$. This also implies that high collagen density is having little effect on vasculature, hence it would be reasonable to assume k_{13} is significantly smaller than k_2, and we take $k_{13} \approx k_2/10$ which gives $k_{13} = 0.0003$ to be consistent with the biology.

$u(M, N) = M/(M + k_{14}) + N/(N + k_{17})$: There is an absence of specific data on blood vessel occlusion so we assume a standard saturating form for our function with parameters corresponding to related observations where possible. For example, at normal levels of macrophages and nitric oxide no occlusion is observed (Kischer *et al.*, 1982), thus $k_{14} >$ average number of macrophages found during normal healing. Hence, we choose k_{14} to be close to the maximum number of macrophages present, thus giving $k_{14} \approx 80$. We apply a similar argument for k_{17}. Our function $s(N)$ which represented blood vessel dilation had 1.6 nM as the nitric oxide concentration which lead to half the maximal dilation. Given that we would expect occlusion to occur when nitric oxide levels are in excess of those required for dilation, leads us to conclude that $k_{17} > 1.6$. So for a provisional estimate we take $k_{17} \approx 2$ nM.

k_{15}: Schaffer *et al.* (1997a) showed that macrophages are a significant source of wound nitric oxide and a production rate of 20.4 nmol μg^{-1} DNA/48 hr was recorded. Applying the approximation for cell DNA content used to calculate f_0 we obtain a value of $k_{15} = 10.2$. This result is in agreement with the data by Iuvone *et al.* (1994), who observed an NO synthesis rate of $\sim$15 nmol per 10^6 cells per 24 hr, which yields $k_{15} \approx 15$.

k_{16}: There is an absence of data on the rate at which fibroblasts produce collagen in response to TGF-β; however there is a comparative study by Ghahary *et al.* (1993) which provides quantitative data on the level of increased responsiveness of hypertrophic fibroblasts to TGF-β. They recorded a 61% increase in TGF-β mRNA in hypertrophic scar samples in comparison to the normal wound tissue. Thus we take k_{16}, 1.61 times larger in our simulations of hypertrophic lesions.

In terms of order of magnitude estimates for this parameter in normal scar tissue we make an approximation based on the timing and duration of wound-healing events. Both nitric oxide and TGF-β are important in fibroblast collagen deposition; however TGF-β predominantly acts during the early phases of repair (Shah *et al.*, 1994), whereas nitric oxide has a sustained influence (Schaffer *et al.*, 1997a). Therefore, this difference in duration of influence leads us to expect that the rate, k_{16}, of TGF-β stimulated collagen

production will be greater than that of NO-stimulated protein synthesis, i.e. $k_{16} > g(N)$. We would expect k_{16} to be of the order of hours since, for example, applying anti-TGF-β 7 days post-wounding was too late to have the anti-scarring properties that were observed with early application (Shah *et al.*, 1994). This partly suggests that the TGF-β effect on collagen deposition is rapid. Given there is no specific data on this rate we are forced to make an estimate of k_{16} based on the more general information we have discussed. Hence, we assume a half-life of 5 hr to fit in with the expected rate of events. This yields a value of $k_{16} = (\ln 2/(5/24)) \approx 3.3$.

d_8: Macrophages are known to exist in the wound for several days after the initial migration; so based on this we take a decay rate for macrophage cells to be of the order of $d_8 \approx 0.2\ \text{day}^{-1}$.

k_8: Maximal chemotactic migration of macrophages into the wound occurs in response to femtomolar (10^{-5} M) concentrations of TGF-β. In particular, Wahl *et al.* (1987) recorded a value of 8 fM ($2 \times 10^{-4}\ \text{ng ml}^{-1}$). By 3 days post-wounding ($t = 0$), TGF-β levels would be significantly higher and macrophage numbers have reached a maximum. Wahl *et al.* (1987) discuss that at these higher levels of TGF-β the recruited macrophages are activated to secrete mitogens, thus we would expect the rate of macrophage recruitment, k_8, to be quite low, so certainly we would have $k_8 T < d_8 M$.

We are able to make an order of magnitude estimate for k_8 by applying the fact that macrophages are principally present during fibroplasia and this phase ends at approximately 20 days post-wounding. Hence, we could estimate a half-life for the removal of the macrophages from the wound to be of the order of 9 days. Applying this to the equation for the macrophage population [eqn (5)] by assuming TGF-β is at an average concentration and given that we know d_8, leads us to the following expression for $M(t)$: $M_0 e^{-d_8 t} + (k_8/d_8)T_a$. Thus, $0.5 \times M_0 = M_0 e^{-d_8 \times 9} + k_8/d_8 \times 1$ (using the approximation for the time it takes for half the macrophages to leave the wound). Given that we had an estimate of 100 macrophage cells mm^{-3} at 3 days post-wounding the expression yields a value of $k_8 \approx 7$.

d_9: Coffey *et al.* (1987) have recorded a plasma half-life of 2–3 min for active TGF-β; this has been confirmed by Wakefield *et al.* (1990). However, the half-life of latent TGF-β is significantly longer, of the order of 110 min (Wakefield *et al.*, 1990). Given this difference it is more realistic to use the latent half-life in our model, because of the continual conversion to active TGF-β which occurs. Wakefield *et al.* (1990) support this assumption in their discussion. Hence, $d_9 = \ln 2/(110/60 \times 24) = 9.1\ \text{day}^{-1}$.

K: A study by Krischel *et al.* (1998) found that fibroblasts undergo cytostasis at concentrations of nitric oxide greater than 0.25 mM (based on the addition of an NO donor every 24 hr).Thus, we would not expect the background nitric oxide production rate, K, to be larger than this, i.e. $K \leqslant 250\,000\ \text{nM day}^{-1}$. However, keratinocytes exhibit increased proliferation in response to NO concentrations between 0.01 and 0.25 mM. Given the thickened epidermis observed in keloids we would predict that $K \geqslant 10000\ \text{nM day}^{-1}$. Thus, we base our choices of K on these observations.

A.4. SENSITIVITY ANALYSIS OF THE FULL MODEL PARAMETERS

Given that the parameters for the full model required more estimation and supposition than the simple model, a sensitivity analysis is particularly important. We carried out a sensitivity analysis, where as in our study of the simple model parameters, S represents the measure of sensitivity and we changed the parameters and initial conditions by $\pm 50\%$. As we can see from Fig. A2, the solution is highly robust to changes in parameters and initial conditions. Figure A2 also demonstrates that the most sensitive parameter in the full model is d_9, which is the decay rate of TGF-β. However, any sensitivity occurred in response to decreases in the parameter which is biologically unrealistic, as we have quite accurate data on d_9 and as discussed earlier we know that it has a maximum half-life of 110 min which gave us our value for the parameter. Biologically, the most we would expect is that the half-life is shorter than 110 min, thus implying that d_9 could be larger. Hence, decreasing d_9 is unrealistic. Thus this supports the robustness of our model further.

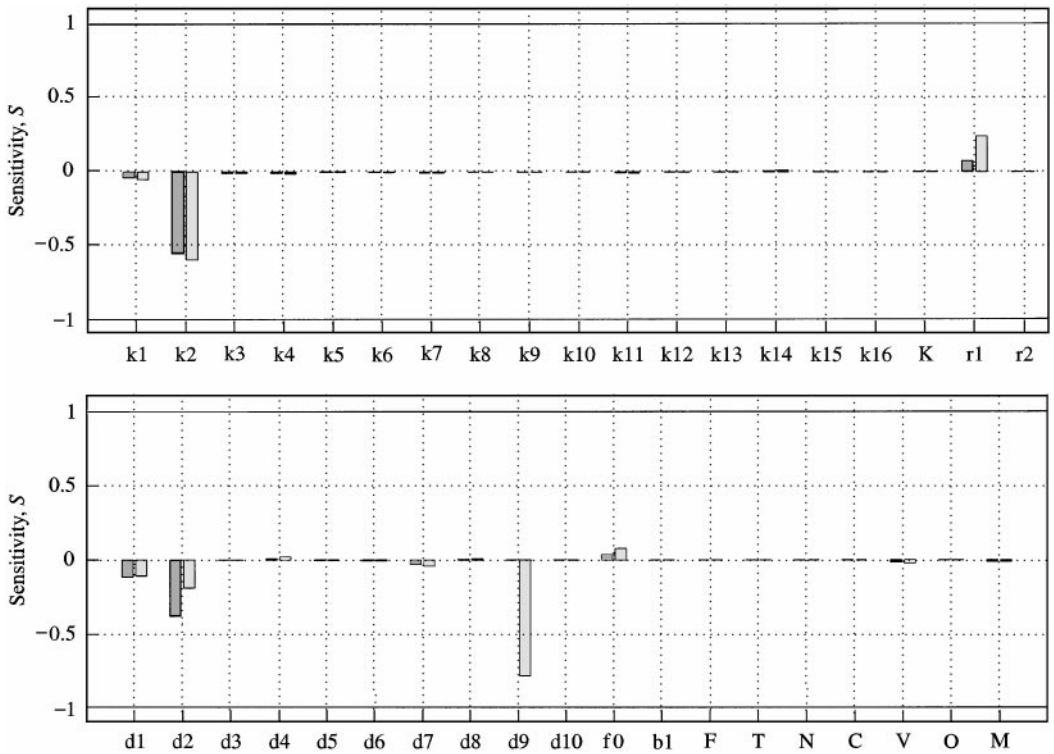

FIG. A2. Bar chart displaying the results of a parameter sensitivity analysis. We varied each parameter and initial condition by $\pm 50\%$ from our fixed set of parameter values which are as follows: $r_1 = 0.92$, $r_2 = 0.5$, $d_1 = 0.12$, $d_2 = 0.000075$, $d_3 = 800$, $d_4 = 3800$, $d_5 = 500$, $d_6 = 20$, $d_7 = 800$, $d_8 = 0.2$, $d_9 = 9.1$, $d_{10} = 0.02$, $k_1 = 0.0004$, $k_2 = 0.006$, $k_3 = 0.5$, $k_4 = 5280$, $k_5 = 4$, $k_6 = 1.2$, $k_7 = 185$, $k_8 = 7$, $k_9 = 0.07$, $k_{10} = 0.015$, $k_{11} = 0.0015$, $k_{12} = 0.01$, $k_{13} = 0.0003$, $k_{14} = 80$, $k_{15} = 12$, $k_{16} = 3.3$, $k_{17} = 2$, $a_1 = 1/300$, $m = 20$, $f_0 = 2.785$, $b_1 = 0.1$ [decay rate of $f(T)$], $K = 0.1$. The initial conditions used are $F(0) = F_0 = 100\,\text{cells}\,\text{mm}^{-3}$, $C(0) = C_0 = 0.1 \times 5.4\,\mu\text{g}\,\text{mg}^{-1}$ dry weight, $N(0) = N_0 = 1$ nM, $O(0) = O_0 = 0.1\%$, $M(0) = M_0 = 100\,\text{cells}\,\text{mm}^{-3}$, $T(0) = T_0 = 1 \times 10^{-2}\,\text{ng}\,\text{mm}^{-3}$ and $V(0) = V_0 = 5$. (These values are discussed further in this section.) The sensitivity measure, S, is the percent change in solution measure (collagen steady-state density, C_s) divided by the percent change in parameter. So on our chart ± 1 reflects a change in output which is in equal proportion to the change in input. Given that all results are bounded by ± 1 it demonstrates that the parameters for the full model are highly robust and supports our choice of values: (■) + 50%; (□) − 50%.